

Evolution of D-branes Under Closed String Tachyon Condensation

Shiraz Minwalla and Tadashi Takayanagi

Jefferson Physical Laboratory

Harvard University

Cambridge, MA 02138

Abstract

We study the evolution of stable D-branes of \mathbf{C}/\mathbf{Z}_n and twisted circle theories in the process of closed string tachyon condensation. We interpret the fractional branes in these backgrounds as type II branes wrapping ('blown up') cycles, and trace the evolution of the corresponding cycles under tachyon condensation. We also study RG flows of the corresponding $\mathcal{N} = 2$ boundary conformal field theories. We find flows along which fractional D-branes either disappear or evolve into other fractional D-branes, and other flows along which bulk branes either disappear or evolve into stable branes.

Contents

1. Introduction	2
2. Twisted Circles, \mathbf{C}/\mathbf{Z}_n and Type 0 theory	6
2.1. Twisted Circles	6
2.2. \mathbf{C}/\mathbf{Z}_n from $R \rightarrow 0$	7
2.3. Type 0 from $n \rightarrow \infty$	8
3. Closed String Tachyon Condensation in Twisted Circles	8
3.1. Decay of Twisted Circles in Gauged Linear Sigma Model Description	9
3.2. A Construction of the Interpolating Liouville Flow	11
3.3. The Classical Geometry of Tachyon Condensation	12
4. D Branes on Twisted Circles, \mathbf{C}/\mathbf{Z}_n and Type 0	14
4.1. D Branes on Twisted Circles	14
4.2. D-Branes on \mathbf{C}/\mathbf{Z}_n	16
4.3. D-Branes in Type 0 Theory	18
4.4. Dirac Quantization	19
5. D-branes Under Tachyon Condensation	21
5.1. Geometrical Analysis	22
5.2. Charge Conservation	24
5.3. GLSM analysis of \mathbf{C}/\mathbf{Z}_n Boundary Flows	25
5.4. GLSM Analysis of Twisted Circle Boundary Flows	33
6. Evolution of D-branes under More General RG Flows	34
7. Discussion	36
Appendix A. Type 0 theory and Interpolating Orbifolds	39
Appendix B. Decay of \mathbf{C}/\mathbf{Z}_n	40
B.1. Review of Tachyon Condensation in \mathbf{C}/\mathbf{Z}_n	40
B.2. Tachyon Condensation using the Gauged Linear Sigma Model Construction	42
B.3. The Sigma Model Limit	43
B.4. GSO Projection	43
B.5. The Sigma Model in the UV	44
B.6. Deviations from the UV Fixed Point	44
B.7. Classical RG flow to the IR	45
B.8. Qualitative Properties of the Exact Flow	46
Appendix C. Classical Metric in Twisted Circle GLSM	47
Appendix D. D-brane Spectrum in dual LG Theory	48
D.1. LG Theory dual to GLSM	48
D.2. Description of D-branes in LG Theory dual to Orbifold	51
D.3. Computation of RR-charges	53
D.4. Speculations on D-branes in the LG Model	54
Appendix E. Useful T-duality Relations	55

1. Introduction

Consider a classical scalar field theory with action

$$S = \int d^d x \frac{1}{2g^2} [(\partial_\mu \varphi)^2 + V(\varphi)] \quad (1.1)$$

where $V(\varphi)$ takes the form shown in Fig. 1. A glance at this action carries a lot of information. For instance, it is immediately clear that this system has at least two classically stable static backgrounds ($\varphi = a$ and $\varphi = c$) and two unstable backgrounds ($\varphi = 0$ and $\varphi = b$). The spectrum around the unstable solution $\varphi = 0$ includes a tachyon; the end point of tachyon condensation process is a gas of radiation about the stable vacuum $\varphi = a$.

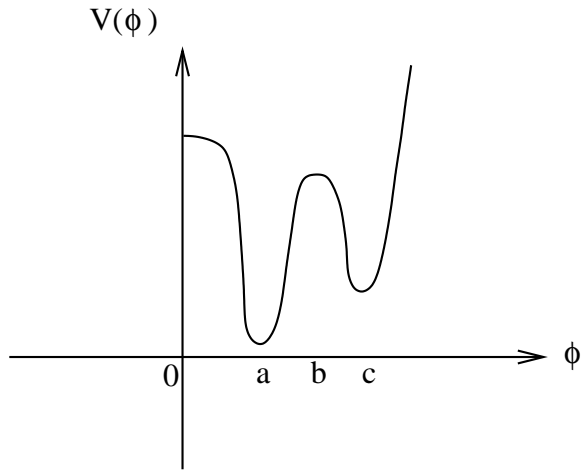


Fig. 1: Configuration space of scalar field theory with potential.

It is instructive to contrast our understanding of the model (1.1) with our current understanding of string theory. We know a great deal about the properties of several particular classical solutions of string theory but lack intuition on the global structure of the configuration space. It is not even clear whether all solutions (e.g. the Bosonic String) are part of the same configuration space.

The recent study of closed string tachyon condensation has begun to address this issue. For example, Adams, Polchinski and Silverstein (APS) [1] have argued that unstable \mathbf{C}/\mathbf{Z}_n orbifolds of type II theory decay to type II theory in flat space, a process roughly analogous to the decay of $\varphi = 0$ to $\varphi = a$ in the model (1.1) described above (see also [2][3][4][5]). Similarly, generalizations of this study indicate that twisted circles or Melvin

compactifications of type II theory [6] decay to supersymmetric circle compactifications of flat space [7] (for recent discussions of closed string tachyon condensation in the twisted circle see also e.g. [8][9][10][11][12]). These decay processes access otherwise unexplored regions of the configuration space of string theory, and deserve to be studied in greater detail. D-branes have often proved to be useful probes in string theory and the unstable backgrounds we study host a rich spectrum of stable D-branes. In this paper we will study how these stable branes evolve in the process of closed string tachyon condensation.¹

Our study will focus largely on twisted circle theories. These rather versatile models appear in a two parameter family labeled by the size of the twisted circle R and the angular twist $2\pi(1 - \frac{1}{n})$ in an auxiliary 2-plane, upon traversing this circle. As we review in section 2 below, twisted circles reduce to \mathbf{C}/\mathbf{Z}_n orbifolds in the limit² $R \rightarrow 0$ [14], and so may be thought of as a desingularization or ‘blow up’ of \mathbf{C}/\mathbf{Z}_n (in particular the \mathbf{C}/\mathbf{Z}_n fractional 0-brane may be ‘blown up’ into a wrapped twisted circle 1-brane). Consequently, twisted circle dynamics reduces to \mathbf{C}/\mathbf{Z}_n dynamics upon taking the appropriate limit.

We study the evolution of D-branes under tachyon condensation using two complementary approaches. Our first approach uses the remarkable fact that the Euclidean (more precisely Liouville) evolution of twisted circle models is approximately captured by an easily obtained and completely smooth interpolating geometry, a space that is similar in some respects to Taub Nut space. In order to take advantage of this fact, we interpret the D-branes on twisted circle backgrounds as usual type II branes wrapping various geometric cycles of the twisted circle background. We then follow the evolution of these cycles to late Euclidean ‘time’ in the interpolating RG-flow geometry. We find that the cycles wrapped by twisted circle D-branes always evolve, under RG flow in one of three distinct ways.

1. In some cases the relevant cycle remains nonsingular through the process of RG flow and smoothly evolves into a nontrivial cycle in the IR geometry. This allows us to unambiguously trace the evolution of the corresponding D-brane under tachyon

¹ See [13] for a discussion of similar issues in the context of nonsupersymmetric $\mathbf{C}^2/\mathbf{Z}_n$ orbifolds.

² Intriguingly they also reduce to orbifolds of type 0 theory in the limit $n \rightarrow \infty$; however the smoothness of this limit is open to debate.

condensation. For example we conclude that the twisted circle 3-brane evolves into the usual type II 3-brane (a similar result is true of the 2-brane of \mathbf{C}/\mathbf{Z}_n).

2. In other cases, the relevant cycle shrinks to zero size at a particular Euclidean time, and remains trivial through the subsequent RG flow. This happens only at the fixed point (or the origin) of the orbifold. In these cases (which includes the twisted circle fractional 1-brane and so the \mathbf{C}/\mathbf{Z}_n fractional 0-brane) we conjecture the existence of flows along which the corresponding D-brane simply disappears at some finite time during RG flow.
3. Most interestingly, in some cases the relevant cycle degenerates at exactly one point in the full RG flow geometry (intuitively, this cycle is non vanishing both before and after the singular point $r = 0$). In such cases we conjecture the existence of two qualitatively distinct RG-flows (precisely which one is implemented depends on the details of the initial conditions). Along the first kind of flow the corresponding D-brane disappears when its cycle degenerates. Along the second kind of flow the D-brane evolves, through the singularity, and eventually wraps the corresponding smooth cycle in the supersymmetric space. For example, we conjecture that the twisted circle bulk 1-brane (resp the \mathbf{C}/\mathbf{Z}_n bulk 0-brane) can either disappear near the origin, or evolve into a 1-brane wrapping the supersymmetric circle (resp bulk 0-brane on \mathbf{C}) under the process of tachyon condensation.

Geometrical considerations also lead us to conjecture the existence of flows in which certain bulk branes (e.g. a D1-brane wrapped on a compactified circle in flat space) are created out of nothing, in the process of tachyon condensation. Finally the flows we have described above may be superposed to produce more complicated flows (e.g. one in which a fractional brane is disappears, while at the same time a bulk brane is created out of nothing).

We are able to confirm some of these geometrically inspired conjectures using a more rigorous approach. Recall that [3] and [7] were able to obtain exact results on closed string tachyon condensation by studying $\mathcal{N} = 2$ supersymmetric renormalization group flows in Gauged Linear Sigma Models (GLSMs). Introducing D-branes into the story

corresponds to putting the GLSMs on the disk with appropriate boundary conditions and adding relevant boundary degrees of freedom (‘Chan Paton factors’) [15][16][17]. When the boundary conditions and interactions in question also preserve $\mathcal{N} = 2$ supersymmetry, it is not difficult to construct RG flows that follow the evolution of these boundary conditions to late Euclidean times. Using this method, we are able to construct examples of all the flows described in items 1-3 above, including both kinds of flows described in item 3. As one check on the formal reasoning in this part of the paper, we present (following [1] and [18] in the absence of boundaries) an explicit solution to the 1-loop beta function equations that describes the \mathbf{C}/\mathbf{Z}_n 2-brane relaxing to the supersymmetric 2-brane in flat space.

As we have noted, D-branes disappear along some of the flows described above. Interestingly this disappearance occurs, roughly, via a process of open-string tachyon condensation (even though the branes under study were stable in the UV). This open string instability is triggered (at some finite Euclidean time) by the closed string tachyon condensation process (see sections 5 and 7 for more details).

We have, so far, described the evolution of D-branes under generic bulk RG flows, along which twisted circles and \mathbf{C}/\mathbf{Z}_n decay to flat space. As is well known, world sheet $N = 2$ supersymmetry guarantees the existence of more fine tuned RG flows in both these models; for instance flows from \mathbf{C}/\mathbf{Z}_n to \mathbf{C}/\mathbf{Z}_m ($n > m$). It is not difficult to repeat the analysis described above on these fine tuned flows. As above we find the geometrically motivated conjectures as to the fate of these D-branes are always borne out by a more rigorous analysis of these flows. In particular, the flows describing the evolution of a single fractional D-branes are always of type described in item 2 above. Some multi-fractional branes fall into the category of item 3; such branes either disappear or evolve into specific other fractional branes under closed string tachyon condensation. The story with bulk branes is unchanged. The analysis of these special flows is particularly useful as it permits a better understand of how geometrical information is encoded in corresponding boundary interactions due to open string tachyon fields.

This paper is organized as follows. In section 2 we review the closed string backgrounds of interest to this paper, namely twisted circles, \mathbf{C}/\mathbf{Z}_n orbifolds and type 0 theory. In section 3 we review the tachyon condensation of twisted circle models [7] and derive

a smooth interpolating Euclidean 4-geometry that approximately captures this tachyon condensation, and study it in detail. In section 4 we review the D-branes in twisted circle backgrounds, and interpret them as usual D-branes wrapping nontrivial cycles in the twisted circle background. We also demonstrate that these branes reduce, in the appropriate limits, to the D-branes of \mathbf{C}/\mathbf{Z}_n and type 0 theory. In section 5 we study the evolution of stable D-branes under tachyon condensation in the models introduced above from two different viewpoints. In section 6 we consider evolution of D-branes under closed tachyon condensation via more general decay channels of the twisted circles and orbifolds. In Appendix A we review the so called ‘interpolating orbifold’ (which interpolates between type II and type 0 string theory). In Appendix B we give a detailed review of closed string tachyon condensation in \mathbf{C}/\mathbf{Z}_n and its description by gauged linear sigma model with some new results. In Appendix C we compute the classical sigma model metric of gauged linear sigma model for the twisted circle. In Appendix D we discuss D-branes in the Landau-Ginzburg (LG) models which are dual to our models. In Appendix E we present a useful list of T-duality relations of twisted circle.

2. Twisted Circles, \mathbf{C}/\mathbf{Z}_n and Type 0 theory

As we have explained in the introduction, in this paper we will study the evolution of stable D-branes in the decay of particular unstable closed string backgrounds. In this section we introduce these unstable backgrounds; Twisted Circles, \mathbf{C}/\mathbf{Z}_n and type 0 theory. We will emphasize that two of these backgrounds, namely \mathbf{C}/\mathbf{Z}_n and type 0 may be realized as specific limits of the Twisted Circle theory.

2.1. Twisted Circles

Consider type II theory in flat ten-dimensional space $(\vec{x} \in \mathbf{R}^{6+1}, y \in \mathbf{R}, z \in \mathbf{C})$, quotiented by a circle identification accompanied by a rotation in an auxiliary plane

$$(\vec{x}, y, z) \sim (\vec{x}, y + 2\pi R, e^{2\pi i\zeta} z). \quad (2.1)$$

We will refer to such a space (or the non-trivial three-dimensional part of it) as a “twisted circle” with radius R . Note that the particular case $\zeta = 0$ corresponds to the usual supersymmetric circle compactification, while $\zeta = 1$ is a circle compactification accompanied by a 2π rotation in a transverse plane, i.e. a Scherk-Schwarz compactification.

Twisted sectors of (2.1) are strings that wind around the y direction and are simultaneously constrained to rotate in an arc on the z plane. As the squared length of such strings grows like r^2 , generic twisted sector states are localized to the origin of the z plane. The exact spectrum of type II theory on twisted circles is not difficult to derive ([6,19,20]; see [14,7] for a brief review.) and confirms these qualitative expectations.

For technical reasons we will restrict ourselves in this paper to the study of (2.1) with a discrete set of twists; $\zeta = (n + 1)/n$ with n odd i.e.

$$(\vec{x}, y, z) \sim (\vec{x}, y + 2\pi R, e^{2\pi i \frac{n+1}{n}} z). \quad (2.2)$$

Note that $2\pi n\zeta = 2\pi(n + 1) \approx 0$. Consequently it is best to think of (2.2) as a \mathbf{Z}_n orbifold $(\mathbf{C} \times \mathbf{S}^1)/\mathbf{Z}_n$ of a supersymmetric circle compactification

$$(\vec{x}, y, z) \sim (\vec{x}, y + 2\pi nR, z), \quad (2.3)$$

of type II theory. States in the twisted sector of the \mathbf{Z}_n orbifold are all localized on \mathbf{C} while states in the untwisted sector are the usual winding and Kaluza Klein modes on (2.3) and are delocalized.

At large R all twisted sector states are very massive and so (2.2) is classically stable. On the other hand, it turns out that (2.2) is unstable at small R ; more precisely, the spectrum includes at least one tachyon if and only if $2\alpha'(\frac{n-1}{n}) > R^2$; the mass of this state is $M^2 = (R/\alpha')^2 - 2\alpha'(\frac{n-1}{n})$. In this paper, we will be interested in (2.2) in its unstable regime.

2.2. \mathbf{C}/\mathbf{Z}_n from $R \rightarrow 0$

In the limit $R \rightarrow 0$ (2.2) reduces to a simpler \mathbf{Z}_n orbifold of (2.3) [14].

$$(\vec{x}, y, z) \sim (\vec{x}, y, e^{2\pi i \frac{n+1}{n}} z); \quad (2.4)$$

i.e. the usual \mathbf{C}/\mathbf{Z}_n orbifold in a plane transverse to the circle compactification. Note that the winding number of strings around the twisted circle in (2.2) is conserved; this conservation law modulo n reduces to the ‘quantum symmetry’ of the \mathbf{Z}_n orbifold (2.4). (Recall that the \mathbf{Z}_n quantum symmetry of a \mathbf{Z}_n orbifold [21] is generated by an element h defined by the action

$$h : |k\rangle \rightarrow e^{\frac{2\pi ik}{n}} |k\rangle, \quad (2.5)$$

where $|k\rangle$ is any state in the k^{th} twisted sector).

In summary, the $R \rightarrow 0$, the IIA/B twisted circle model (2.2) reduces to IIA/B theory on $\mathbf{R}^7 \times \mathbf{C}/\mathbf{Z}_n$ times a zero size circle, or (by T-duality) to IIB/A theory on $\mathbf{R}^8 \times \mathbf{C}/\mathbf{Z}_n$ [14].

2.3. Type 0 from $n \rightarrow \infty$

In the limit $n \rightarrow \infty$, IIA theory on (2.2) reduces to IIA theory on a Scherk Schwarz circle, i.e. IIA theory modded out by $(-1)^{F_s} \times \sigma$ where σ is the translation $y \rightarrow y + 2\pi R$ and F_s is the space time fermion number. This Scherk Schwarz compactification of type II theory has been referred to as an ‘interpolating orbifold’ [22], as it interpolates between IIA theory on \mathbf{R}^{10} (as $R \rightarrow \infty$) and 0B theory on \mathbf{R}^{10} (as $R \rightarrow 0$). (See Appendix A for more details). Consequently, one may obtain type 0B/A theory from the twisted circle of IIA/B theory by first taking $n \rightarrow \infty$ and then taking $R \rightarrow 0$ [7].

3. Closed String Tachyon Condensation in Twisted Circles

The backgrounds described in section 2 are all unstable; their spectrum includes at least one closed string tachyon. In this section, first we review the tachyon condensation³ of twisted circle theories [7]. After that we derive and study the smooth ‘classical’ Euclidean 4-geometry of the corresponding tachyon condensation process in detail. The intuition we gain from this study will prove useful to us in section 5 below.

³ Recall \mathbf{C}/\mathbf{Z}_n and type 0 theories may be obtained as limits of twisted circle theories.

3.1. Decay of Twisted Circles in Gauged Linear Sigma Model Description

In this subsection we will review a construction of a renormalization group flow that describes the tachyon condensation of twisted circles [7]. The construction of this renormalization group flow uses $\mathcal{N} = (2, 2)$ gauged linear sigma models [23][24] (see [7] and references therein for all details) and is similar to Vafa's construction [3] of a flow for \mathbf{C}/\mathbf{Z}_n (reviewed in detail in Appendix B).

Consider a gauged linear sigma model that contains two charged superfields Φ_1 and Φ_{-n} that transform under $U(1)$ gauge transformations as

$$\Phi_1 \rightarrow e^{i\alpha}\Phi_1, \quad \Phi_{-n} \rightarrow e^{-in\alpha}\Phi_{-n}, \quad (3.1)$$

together with an axionic field $P = P_1 + iP_2$ whose gauge transformation (see [24] for general arguments) is

$$P \rightarrow P + i\alpha. \quad (3.2)$$

Note that P_1 , the real part of P , effectively plays the role of a dynamical FI term. As in B.2, the low energy dynamics is described by a quantum corrected sigma model on the supersymmetric manifold of zero-energy configurations satisfying (D-term condition)

$$-\frac{D}{e^2} = |\varphi_1|^2 - n|\varphi_{-n}|^2 + kP_1 = 0, \quad (3.3)$$

modulo gauge equivalences, where k is the coefficient of the kinetic term of the P field (see [7])⁴.

At large values of P_1 (UV region), we use the gauge freedom to set φ_{-n} to be real and positive, and then use (3.3) to solve for φ_{-n} as $\varphi_{-n} = \sqrt{(|\varphi_1|^2 + kP_1)/n}$. Plugging this into the classical action (see Appendix C for details) we obtain the flat sigma model on the complex plane \mathbf{C} (parameterized by φ_1) times a cylinder (parameterized by P) orbifolded by the unfixed \mathbf{Z}_n gauge symmetry

$$\varphi_1 \rightarrow e^{2\pi i/n}\varphi_1, \quad P_2 \rightarrow P_2 + \frac{2\pi i}{n}. \quad (3.4)$$

⁴ More precisely, we study the gauged linear sigma model modded out by a discrete non anomalous R symmetry (see B.3). This modding out imposes the type II GSO projection on the low energy sigma model.

Consequently, at large P_1 , dynamics reduces to that of a sigma model on the twisted circle theory $(\mathbf{C} \times \mathbf{S}^1)/\mathbf{Z}_n$ with a circle of radius $R_{UV} = \frac{\sqrt{\alpha'k}}{n}$. Its metric is given by

$$ds^2 = (d\rho)^2 + \rho^2(d\theta)^2 + \frac{k}{2}(dP_1)^2 + \frac{k}{2}(dP_2)^2, \quad (3.5)$$

where θ is the angle of⁵ φ_1 and we defined $\rho = |\varphi_1|$.

In [7] it is argued that P_1 may be regarded as a Liouville or scale direction, with $P_1 \rightarrow \infty$ corresponding to the UV. Consequently, the evolution of our target space in the P_1 mimics the flow of the energy scale from UV to IR as the change of P_1 from $P_1 = \infty$ to $P_1 = -\infty$. In this sense the coordinate $-P_1$ can be regarded as the real time t after the Wick rotation. Consequently, the end point of tachyon condensation in the twisted circle theory is captured by the behavior of the sigma model as $P_1 \rightarrow -\infty$. In this limit we obtain the cylindrical flat space $\mathbf{C} \times \mathbf{S}^1$ with radius $R_{IR} = \sqrt{\alpha'k}$

$$ds^2 = d\rho'^2 + n^2\rho'^2(d\theta)^2 + \frac{k}{2}(dP_2 - d\theta)^2, \quad (3.6)$$

where we defined $\rho' = |\varphi_{-n}|$. Thus we conclude that the twisted circle theory decays into a supersymmetric circle compactification of flat space.

Now consider the limit $k \rightarrow 0$; the twisted circle reduces to the orbifold $\mathbf{C}/\mathbf{Z}_n \times \mathbf{S}^1$, where the radius R' of this \mathbf{S}^1 is n times the radius R of the twisted circle background [14]. According to (3.6), the end point of this decay is $\mathbf{C} \times \mathbf{S}^1$, where the radius of \mathbf{S}^1 is given by $nR = R'$. Consequently, the decay of $\mathbf{C}/\mathbf{Z}_n \times \mathbf{S}^1$ replaces the orbifold by flat space, and leaves the \mathbf{S}^1 untouched, consistent with the conclusions of [1] [3](for completeness we review tachyon condensation in \mathbf{C}/\mathbf{Z}_n in detail in Appendix B).

In the limit $n \rightarrow \infty$ of the twisted circle reduces to a \mathbf{Z}_2 orbifold of type 0 theory on a circle of radius $\frac{\alpha'}{R}$ (see previous section). If the description of tachyon condensation commutes with $n \rightarrow \infty$ (and it is not clear that it does), it follows that the end point of tachyon condensation of the \mathbf{Z}_2 orbifold of type 0A/B theory on an \mathbf{S}^1 (reviewed in subsection 2.3) is simply type IIB/A theory on \mathbf{R}^{10} .

⁵ In Appendix C we denote this angle by θ_1 just for notational convenience. Both are the same.

3.2. A Construction of the Interpolating Liouville Flow

As we have reviewed in the previous subsection, the entire process of tachyon condensation of the twisted circle theory is described by a conformal field theory. The CFT that captures the details of this tachyon condensation process may be constructed via a two step procedure. In the first step we plug the D-term equation (3.3) into the GLSM action, fix the $U(1)$ gauge and then integrate out the (massive) gauge field which appears quadratically in the Lagrangian. These manipulations are easy to perform and lead, in the sigma model limit $e \rightarrow \infty$ to a $\mathcal{N} = (2, 2)$ sigma model on a smooth four dimensional target space⁶ (see Appendix C for details)

$$ds^2 = d\rho^2 + d\rho'^2 + \frac{2}{k}(n\rho'd\rho' - \rho d\rho)^2 + \frac{\frac{k}{2}\rho^2 d\tilde{\theta}_1^2 + \frac{k}{2}\rho'^2 d\tilde{\theta}_2^2 + \rho^2 \rho'^2 (nd\tilde{\theta}_1 + d\tilde{\theta}_2)^2}{\rho^2 + n^2 \rho'^2 + \frac{k}{2}}. \quad (3.7)$$

The coordinates that appear in (3.7) are related to those in (3.5) and (3.6) by $\tilde{\theta}_1 \equiv \theta - P_2$ and $\tilde{\theta}_2 = nP_2$. (3.4) implies that $\tilde{\theta}_{1,2}$ are periodic with periodicity 2π , and that the radial parameters ρ and ρ' run from 0 to ∞ .

In the next (and unsatisfyingly implicit) step of this construction we flow to the IR of this sigma model to obtain the desired CFT. Unfortunately, we have not been able to find an exact description of the resulting $\mathcal{N} = (2, 2)$ SCFT. However, in this paper we will be interested only in qualitative aspects of (3.7). We will assume that, as in [24], (and several earlier analysis of Calabi Yau constructions, see for instance [23]), the asymptotic geometry and topology contained in the exact SCFT match those of (3.7). In the rest of this section we will study the geometry of (3.7) (we refer to (3.7) as the ‘classical’ geometry of tachyon condensation).

⁶ Here we again set the angle of the complex scalar field φ_{-n} to zero by gauge fixing. We can also employ a gauge invariant expression without gauge fixing, which looks more complicated. Since the result does not change, we will use the former expression. We thank K.Hori very much for comments on this point.

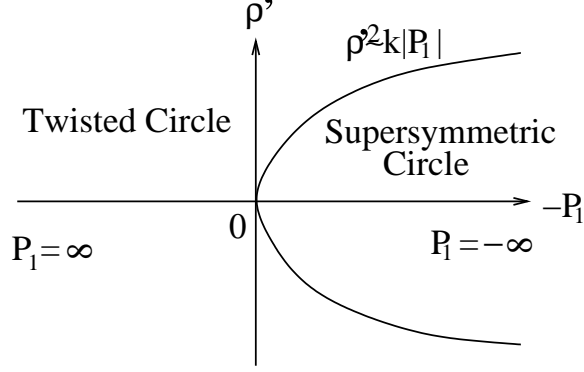


Fig. 2: Geometry change under the closed string tachyon condensation. The bubble of flat space appears at the origin when $P_1 = 0$. Later it will expand and finally it covers the whole space.

3.3. The Classical Geometry of Tachyon Condensation

As we have argued above, (3.7) describes a space that interpolates between the twisted circle geometry and flat space. It is easy to see this in detail. Rewriting the metric in terms of the coordinates ρ , θ , P_1 and P_2 ; see around (3.2)- (3.6) for notation) we find that, in the UV limit ($P_1 \gg 0$) the interpolating space reduces to the twisted circle (3.5)

$$\begin{aligned}
ds^2 &= (d\rho)^2 + \frac{k}{2}(dP_1)^2 + \frac{(\rho d\rho + \frac{k}{2}dP_1)^2}{n(\rho^2 + kP_1)} \\
&+ \frac{(n\rho^4 + (nkP_1 + \frac{k}{2})\rho^2)(d\theta)^2 - k\rho^2(d\theta)(dP_2) + \frac{k}{2}((n+1)\rho^2 + nkP_1)(dP_2)^2}{(n+1)\rho^2 + nkP_1 + \frac{k}{2}}. \quad (3.8) \\
&\approx (d\rho)^2 + \rho^2(d\theta)^2 + \frac{k}{2}(dP_1)^2 + \frac{k}{2}(dP_2)^2 \quad (P_1 \gg 0).
\end{aligned}$$

On the other hand, rewriting the metric in terms of the coordinates ρ' , θ , P_1 and $\tilde{\theta}_1$, we see that the interpolating space reduces to flat space (3.6) (i.e. supersymmetric circle) in the IR ($P_1 \ll 0$)

$$\begin{aligned}
ds^2 &= (d\rho')^2 + \frac{k}{2}(dP_1)^2 + \frac{(n\rho'd\rho' + \frac{k}{2}dP_1)^2}{n\rho'^2 + kP_1} \\
&+ \frac{\frac{k}{2}(n\rho'^2 + kP_1)(d\tilde{\theta}_1)^2 + n^2\rho'^2(n\rho'^2 + kP_1)d\theta^2 + \frac{kn^2}{2}\rho'^2(d\tilde{\theta}_1 - d\theta)^2}{n(n+1)\rho'^2 + kP_1 + \frac{k}{2}} \quad (3.9) \\
&\approx d\rho'^2 + n^2\rho'^2(d\theta)^2 + \frac{k}{2}(d\tilde{\theta}_1)^2.
\end{aligned}$$

In greater detail, (3.7) represents the decay of the twisted circle background via the nucleation and growth of a bubble of supersymmetric S^1 compactification. This bubble is

nucleated at ‘time’ $P_1 = 0$ (and at $\rho = \rho' = 0$). The radius R_b of this nucleated bubble (see Fig.2) grows in time like $R_b \sim \sqrt{-kP_1}$ (this diffusive growth⁷ matches the behavior observed in [1], [18]). These results precisely show the expected behavior of the tachyon condensation process (see Appendix B.1 for a general discussion).

In order to understand the transition between the twisted circle and supersymmetric geometry, it is useful to focus on the point at which the bubble of supersymmetric circle is first nucleated, i.e. the neighborhood of $P_1 = \rho = \rho' = 0$. (3.7) reduces to

$$ds^2 = d\rho^2 + \rho^2 d\tilde{\theta}_1^2 + d\rho'^2 + \rho'^2 d\tilde{\theta}_2^2, \quad (3.10)$$

i.e. (smooth) polar coordinate of \mathbf{R}^4 .

It is interesting to trace the behavior of various cycles in the twisted circle, as the space transforms itself from the twisted circle to flat space. The twisted circle \mathbf{S}_A^1 defined by (see Fig.3)

$$\mathbf{S}_A^1 : (\rho, \theta, P_2) = (0, s_1, s_1), \quad 0 \leq s_1 \leq 2\pi/n, \quad (3.11)$$

which is non contractible for $P_1 \gg 0$ (UV region), shrinks and disappears at $P_1 = 0$. This is simply the angle circle $\tilde{\theta}_2$ of one of the two planes in (3.10). This cycle becomes trivial for $P_1 < 0$.

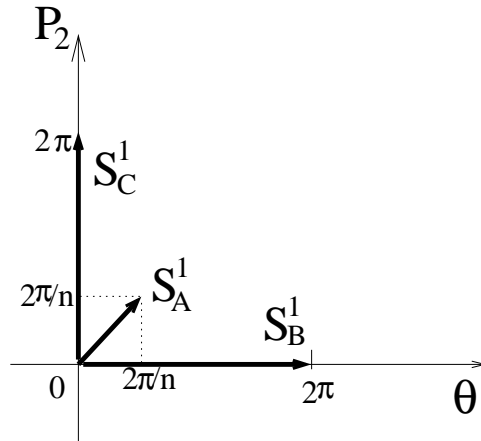


Fig. 3: One cycles in twisted circle.

⁷ In order to see this note that, in the far region $\rho'^2 \gg k|P_1|$ (3.7) reduces to the twisted circle, while in the opposite limit $\rho'^2 \ll k|P_1|$ we get the flat space (3.6). $\rho'^2 \approx k|P_1|$ (see Fig.2) represents a transition between these regions.

It is also interesting to track the evolution of the supersymmetric circle \mathbf{S}_B^1 defined by

$$\mathbf{S}_B^1 : (\rho, \theta, P_2) = (0, s_2, 0), \quad 0 \leq s_2 \leq 2\pi, \quad (3.12)$$

back in ‘time’, from the IR to the UV. This cycle (see Fig.3) also vanishes at $P_1 = 0$; in fact it is simply the other angle $\tilde{\theta}_1$ in (3.10).

In section 5 below we will be interested in the third cycle (see Fig.3)

$$\mathbf{S}_C^1 : (\rho, \theta, P_2) = (a, b, u), \quad 0 \leq u \leq 2\pi, \quad a, b = \text{constant} \quad (3.13)$$

which winds n times around the twisted circle in the UV $P_1 \gg 0$ and winds once around the supersymmetric circle in the IR $P_1 \ll 0$. Note that this cycle vanishes at the point $\rho = P_1 = 0$.

4. D Branes on Twisted Circles, \mathbf{C}/\mathbf{Z}_n and Type 0

The spectrum of D-branes on Twisted circles has been previously derived using a boundary state analysis [25] [26]. In this section we will review the results, and provide a spacetime interpretation of these branes. We will also describe how these branes reduce, in the appropriate limits, to the branes of \mathbf{C}/\mathbf{Z}_n and type 0 theory.

4.1. D Branes on Twisted Circles

D branes on twisted circle backgrounds are of two sorts; those that live at a point on the twisted circle, and those that wrap around the twisted circle.

A branes at a point on the twisted circle is best thought of as an array of branes on the covering space (see, for instance [27]). At low energies such branes behave much like their counterparts in type II theory on flat space.

D branes that wrap the twisted circle are more interesting. Consider a 1-brane that wraps the twisted circle once. As in the case of twisted sector strings, such a brane is confined to the origin of the z plane. Classically, its mass is given simply by the usual D1-brane tension times the minimum length of the twisted circle $M = \frac{R}{g\alpha'}$. Of course such

1-branes actually appear in degenerate one parameter family of solutions labeled by the Wilson line $\theta = \int A \cdot dl \in [0, 2\pi)$ along the brane.

As we have discussed above, the twisted circle may be regarded as a \mathbf{Z}_n orbifold of (2.3), a circle of radius nR . The 1-brane of the previous paragraph is ‘S-dual’ to a twisted sector string state of this orbifold; it is called a fractional brane. On the other hand a 1-brane wrapping the twisted circle n times is the analogue of an untwisted sector string state, and is referred to as a bulk brane. We will now argue that the bulk 1-brane may be thought of as a collection of n fractional 1-branes, with a distribution of Wilson lines. Refer to [28][29] for original literature on (fractional) D-branes in supersymmetric orbifolds (e.g. $\mathbf{C}^2/\mathbf{Z}_n$).

A collection of n fractional 1-branes is described, at low energies, by a 1 + 1 dimensional $U(N)$ gauge theory, with adjoint matter fields Z , ψ and ϕ , where Z represents the position of the brane in the z plane, ψ is the corresponding fermion, and ϕ represents all other massless fields (the gauge field, fluctuations in R^7 plus corresponding fermions). In the vacuum describing n separate 1-branes, these adjoint fields obey the boundary conditions⁸

$$\begin{aligned} Z(2\pi R) &= e^{\frac{2\pi i(n+1)}{n}} S Z(0) S^{-1}, \\ \psi(2\pi R) &= e^{\frac{2\pi i(n+1)}{2n}} S \psi(0) S^{-1}, \\ \phi(2\pi R) &= S \phi(0) S^{-1}. \end{aligned} \tag{4.2}$$

where S is a gluing $U(n)$ matrix representing the Wilson line on the brane. Different values of S represent different classical vacua of this system. In particular $S = I$ represents a configuration of n strings, independently winding the twisted circle. On the other hand, when S is chosen as the shift matrix, the n 1-branes are effectively strung together into a bulk brane; a single brane winding the circle n times. As the shift matrix has eigenvalues

$$e^{\frac{2\pi i k}{n}}, \quad k = 1 \dots n. \tag{4.3}$$

⁸ In the full string theory

$$\chi(2\pi R) = e^{\frac{2\pi i k(n+1)}{n}} C \chi(0) C^{-1} \tag{4.1}$$

where $k = n_z - n_{\bar{z}} + \frac{1}{2}(n_\psi - n_{\bar{\psi}})$, where $n_z, n_{\bar{z}}, n_\psi, n_{\bar{\psi}}$ respectively represent the number of Z, \bar{Z}, ψ and $\bar{\psi}$ open string oscillators excited in producing the open string field χ .

we conclude that bulk 1-brane is simply a collection of n fractional 1-branes with a relative collection of Wilson lines given by (4.3).

Wrapped 3-branes on the twisted circle are rather similar to 1-branes. Consider a single space-filling brane in the twisted circle background. Gauge fields on a collection of n such D3-brane, obey the boundary conditions

$$\begin{aligned} Z(y + 2\pi R, e^{\frac{2\pi i}{n}} z) &= e^{\frac{2\pi i(n+1)}{n}} CZ(y, z)C^{-1} \\ \psi(y + 2\pi R, e^{\frac{2\pi i}{n}} z) &= e^{\frac{2\pi i(n+1)}{2n}} C\psi(y, z)C^{-1} \\ \phi(y + 2\pi R, e^{\frac{2\pi i}{n}} z) &= C\phi(y, z)C^{-1} \end{aligned} \tag{4.4}$$

where the fields have the same meaning as in (4.2) and C is the Wilson Line⁹. When C is the shift matrix, the n ‘fractional’ 3-branes are strung together into a single 3-brane winding the circle n times, i.e. a bulk 3-brane.

Finally, it is easy to verify the absence of 2-branes that wrap the twisted circle $m < n$ times, as no such brane is flat in the covering space. It is, of course, not difficult to construct bulk 2-branes which wrap the twisted circle a multiple of n times.

4.2. D-Branes on \mathbf{C}/\mathbf{Z}_n

We now study the D-branes described in the previous section, in the limit $R \rightarrow 0$. According to subsection 2.2, these branes must reduce to D-branes of $\mathbf{C}/\mathbf{Z}_n \times \mathbf{S}^1$. In this subsection we will explain how this works in detail.

Consider a unit fractional 1-brane of the twisted circle theory, in the limit $R \rightarrow 0$. Such a brane wraps once around the twisted circle (of radius R), and so in some sense, wraps $\frac{1}{n}$ of the larger \mathbf{S}^1 factor in $\mathbf{C}/\mathbf{Z}_n \times \mathbf{S}^1$, see subsection 2.2. We will now argue that there are n different flavors of this 1-brane.

Consider two unit fractional 1-branes of the twisted circle theory, with relative Wilson line θ . Open string modes stretching between these two branes are charged under the relative gauge field, and so obey boundary conditions (4.1) with $C\chi(0)C^{-1} = e^{i\theta}\chi(0)$. When $\theta = 0$, only open string modes with $k = 0 \pmod n$ (k is defined in (4.1)) survive

⁹ The pure gauge configuration corresponding to (for instance) a U(1) Wilson lines is $(A_y, A_z, A_{\bar{z}}) = (\frac{\theta}{2\pi R}, 0, 0)$.

the $R \rightarrow 0$ limit. At generic values of θ all modes are infinitely massive. However, in the neighborhood of $2\pi\theta = \frac{m}{n}$, a new set of modes become massless, namely those with $k = m \bmod n$. Consequently, there are n species of 1-branes that can communicate with the $\theta = 0$ brane; branes with $\theta = \frac{2m\pi}{n} + \mathcal{O}(R)$ where m runs between 0 and $n - 1$.

These results are easier to visualize upon T-dualizing along the \mathbf{S}^1 factor of $\mathbf{C}/\mathbf{Z}_n \times \mathbf{S}^1$. The stretched one branes of the previous paragraphs turn approximately into usual 0-branes on a circle of size $R' = \frac{\alpha'}{nR}$. Turning on a relative Wilson line θ corresponds to separating the branes by $\Delta y = \theta\alpha'/R = \theta nR'$. In taking θ from 0 to $2\pi/n$ we take one of the 0-branes once around the circle; that process converts it into a zero brane of another variety! Repeating this operation produces yet another zero brane, but, upon repeating the process n times we revert to the initial state.

Below we will find use for an operator Q whose action is to transport a zero brane once around the circle (in T-dual language Q shifts the Wilson line by $e^{\frac{i2\pi}{n}}$). If the n distinct 0-branes are denoted by $|i\rangle$, then clearly $Q|i\rangle = |i + 1\rangle$.

In $\mathbf{C}/\mathbf{Z}_n \times \mathbf{R}^8$ (the formal result of taking R to zero on the twisted circle theory) the n distinct species of 0-branes are completely distinct; they cannot be continuously deformed into each other; restated \mathbf{C}/\mathbf{Z}_n has n distinct fractional 0-branes. However the operator Q of the previous paragraph is well defined as $R \rightarrow 0$ and reduces to the generator h of the quantum symmetry (2.5) of \mathbf{C}/\mathbf{Z}_n in the limit¹⁰ and so we conclude that the fractional 0-branes are related to each other by the action of the quantum symmetry. It is well known that \mathbf{C}/\mathbf{Z}_n does indeed have n fractional 0-branes with these properties. Of course the discussion of this section may be mimicked to derive similar results for 2-branes of \mathbf{C}/\mathbf{Z}_n .

To summarize, we have found that the familiar fractional 0-branes (and 2-branes¹¹) of \mathbf{C}/\mathbf{Z}_n have a simple geometric interpretation upon ‘blowing up’ the \mathbf{C}/\mathbf{Z}_n singularity into a twisted circle; they correspond to 1-branes (resp 3-branes) wrapping the twisted circle. This geometrical intuition will help us understand the fate of fractional 0-branes during tachyon condensation, later in this paper.

¹⁰ This is easily seen; Q generates discrete translations, and so counts discrete moment or discrete windings in the T-dual picture.

¹¹ Note that a single D2-brane in \mathbf{C}/\mathbf{Z}_n should be treated as a fractional D2-brane from the group theoretical viewpoint of [28][29] (belonging to one of n irreducible representations of \mathbf{Z}_n). However, its tension is not fractional but usual value. Thus we will call it just a D2-brane in this paper.

4.3. D-Branes in Type 0 Theory

In the limit $n \rightarrow \infty$, the IIA/B twisted circle turns into a Scherk-Schwarz circle of radius R . As we have reviewed in Appendix A, the T-dual of the Scherk-Schwarz compactification of type IIA/B theory is the \mathbf{Z}_2 orbifold of 0B/A on S^1 of radius $\frac{\alpha'}{R}$, where the \mathbf{Z}_2 is generated by $(-1)^{F_L} \times \sigma'$ and σ' is a shift across half the circumference of the circle. Of course, as $R \rightarrow 0$ this theory reduces locally to 0B/A in flat space.

In the limit $n \rightarrow \infty$ the fractional 1-brane of the twisted circle is simply a D1-brane wrapping the Scherk-Schwarz circle. We will now investigate what happens to this D1-brane upon T-dualizing along this circle.

Recall that flat space string theories with $N = (1, 1)$ world sheet supersymmetry have two 0-brane boundary states with different spin structures denoted by $|+\rangle$ and $|-\rangle$ (e.g. see [30]). These boundary states obey

$$\begin{aligned}
 (-1)^{F_L} |+\rangle &= -|-\rangle, \\
 (-1)^{F_R} |+\rangle &= -|-\rangle, \\
 (-1)^{F_L} |-\rangle &= -|+\rangle, \\
 (-1)^{F_R} |-\rangle &= -|+\rangle
 \end{aligned}
 \tag{4.5}$$

From (4.5) we conclude that

1. The only state invariant under $(-1)^{F_L}$ and $(-1)^{F_R}$ is

$$|+\rangle - |-\rangle;$$

this is the 0-brane of type IIA theory.

2. Any linear combination of

$$|+\rangle \text{ and } |-\rangle,$$

is invariant under $(-1)^{F_L+F_R}$; these are the so called electric and magnetic 0-branes of type 0A theory.

- 3.

$$|+(x)\rangle - |-(x + \pi R)\rangle,$$

(where the (x) in brackets refers to the position of the brane on the circle) is the only combination of 0A zero branes invariant under the \mathbf{Z}_2 orbifold of 0A on a circle of size $2\pi R$, described earlier in this section.

With these facts in mind, it is natural to guess, and easy to verify, that the T-dual of a 1-brane wrapping the thermal IIB circle is the a configuration of electric and magnetic 0-branes described in item 3 above.

4.4. Dirac Quantization

In this subsection we will study the charges of the fractional branes described in the previous subsection, and explain how they are consistent with Dirac quantization. This subsection is a side branch away from the main line of development of this paper. The reader eager to turn to the fate of D-branes under closed string tachyon condensation can skip to the next section.

Consider an action that describes the interaction of 3-form and 7-form field strengths with 1-branes and 5-branes

$$\begin{aligned} S &= C \int d^{10}x F_3^2 + e \int A_2 + g \int A_6 \\ &= C \int d^{10}x F_7^2 + e \int A_2 + g \int A_6, \end{aligned} \tag{4.6}$$

where $F_3 = dA_2$, $F_7 = dA_6$ and $F_7 = *F_3$ and A_2 (resp A_6) is integrated over the world volumes of the 1-branes (resp 5-branes). Dirac quantization imposes the constraint

$$\frac{eg}{C} = 2n\pi, \tag{4.7}$$

on the charges in (4.6). In particular, the minimally charged 1-brane (charge e_0) and 5-brane (charge g_0) obey

$$\frac{e_0 g_0}{C} = 2\pi. \tag{4.8}$$

As an exercise that will be useful later in this subsection, consider the dimensional reduction of (4.6) (with minimally charged 1-branes and 5-branes) on $\mathbf{T}^2 \times \mathbf{S}^1$ where the torus has volume V_2 and the circle has radius R . Let A_1 denote the reduction of A_2 along \mathbf{S}^1 , let A_4 denote the reduction of A_6 along T^2 . The dimensionally reduced action that

governing the interaction of particles (10 dimensional strings wrapping S^1) and 3-branes (10 dimensional 5-branes wrapping the T^2) with A_1 and A_4 is

$$S = C(2\pi R)V_2 \int d^7x F_2^2 + e_0(2\pi R) \int A_1 + g_0 V_2 \int A_4. \quad (4.9)$$

Note, of course, that, as a consequence of (4.8), the charges in (4.9) automatically saturate the 7-dimensional Dirac Quantization constraint $\frac{(e_0 2\pi R)(g_0 V_2)}{C(2\pi R)V_2} = 2\pi$.

We now adapt the exercise of the previous paragraph to a compactification $(\mathbf{T}^2 \times \mathbf{S}^1)/\mathbf{Z}_n$ of the twisted circle background $(\mathbf{C} \times \mathbf{S}^1)/\mathbf{Z}_n$. For clarity consider a specific case; let $n = 3$ and let the z plane in (2.2) be an ‘equilateral 2-torus’ (the complex plane modded out by translation vectors at an angle $\frac{2\pi}{3}$ to each other) of volume V_2 . The 3-volume of this twisted circle background is $2\pi R V_2$. The length of the smallest 1-cycle along the twisted circle is $2\pi R$. The volume of the minimal dual 2-cycle is V_2 for any nonzero R and, as in the previous paragraph, the electric and magnetic charges of the dimensionally reduced 7 dimensional theory automatically obey the Dirac quantization condition¹².

We now turn to the $R \rightarrow 0$ limit of this situation. As we have explained in subsection 2.2, the twisted circle reduces to $\mathbf{T}^2/\mathbf{Z}_3 \times \mathbf{S}^1$ where the radius of the \mathbf{S}^1 is $3R$. Note that the minimal volume 2-cycle along the T^2 in this orbifold has volume $V_2/3$. Further, although the orbifold circle has length $3R$, the effective charge of the wrapped 1-brane (which reduces to the fractional 0-brane as $R \rightarrow 0$), continues to be $e_0 2\pi R$ (that is why this object is a fractional rather than bulk brane) and the effective 7-dimensional action governing the electromagnetic interactions between the 2-brane (i.e. ‘fractional’ 2-brane wrapping a cycle of volume $V_2/3$) and the fractional 0-brane is

$$S = C(2\pi R)V_2 \int d^7x F_2^2 + e_0 2\pi R \int A_1 + g_0 \frac{V_2}{3} \int A_4. \quad (4.10)$$

At first sight (4.10) appears to violate Dirac Quantization (as $\frac{(e_0 2\pi R)(g_0 \frac{V_2}{3})}{C(2\pi R)V_2} = \frac{2\pi}{3} \notin 2\pi\mathbf{Z}$). The resolution to this puzzle is rather instructive. The 2-branes and fractional 1-branes

¹² These arguments explain the phenomenological observation noted in [25] that we cannot find any D-brane in the Twisted Circle which is localized in the circle direction and which becomes a fractional D-brane in the $R \rightarrow 0$ limit. Such a brane, if exists, will break the Dirac quantization rule.

of $\mathbf{T}^2/\mathbf{Z}_3 \times \mathbf{S}^1$ are certainly charged under untwisted RR sector potentials. However they are equally charged under all twisted sector RR 2 form potentials (which are massless for $\mathbf{T}^2/\mathbf{Z}_3 \times \mathbf{S}^1$ but not for the twisted circle theory at any nonzero R). The true phase in taking a fractional 0-brane around the Dirac String attached to the 2-brane is the three times the naive result from (4.10), restoring consistency.

5. D-branes Under Tachyon Condensation

In this section we turn to the main topic of this paper; an investigation of the fate of D-branes under tachyon condensation. Here we consider the evolution of D-branes only under bulk flows that lead to a supersymmetric end point; we postpone the discussion of fine tuned flows to the next section. We will first state our conjectures, and then proceed, in the rest of this section, to provide evidences for them from two different viewpoints.

Twisted circles : Any brane located at a point on the twisted circle evolves into the corresponding brane at a point on the supersymmetric circle. 3-branes that wrap the twisted circle once unambiguously evolve into usual 3-branes that wrap the supersymmetric circle once. All fractional 1-branes disappear in the process of tachyon condensation. A bulk 1-brane (which wraps the twisted circle n times) either disappears (this is possible only near the origin) or evolves into a bulk 1-brane that wraps the supersymmetric circle once.

Orbifold \mathbf{C}/\mathbf{Z}_n : All n varieties of space filling 2-branes evolve into the usual space filling 2-branes in flat space. Every fractional 0-brane disappears in the process of tachyon condensation. A bulk 0-brane either disappears (again this is possible only near the fixed point) or evolves into a usual 0-brane in flat space.

\mathbf{Z}_2 Orbifold of type 0A on \mathbf{S}^1 : It should be emphasized that all results about type 0 theory are obtained upon taking a potentially dangerous $n \rightarrow \infty$ limit. With this caveat in mind, we find the following results. A pair of electric and magnetic D(p+1)-branes wrapping the circle evolve into a single Dp-brane in IIB theory. A pair of diametrically separated electric and magnetic 0-branes disappear in the process of tachyon condensation. On the other hand, diametrically opposed 0A 2-branes 4-branes and 6-branes evolve respectively into single IIB 3-branes, 5-branes and 7-branes.

We will now proceed to provide evidence for these conjectures. The rest of this section is organized as follows. In subsection 5.1 we explain how the results for twisted circle theories follow from topological properties of the interpolating geometry presented in the previous section. Results for \mathbf{C}/\mathbf{Z}_n and type 0 theory follow from the appropriate limits (see section 2 and 3) of the twisted circle theory. In subsection 5.2 we comment on how our results are consistent with charge conservation. In subsection 5.3 and 5.4, respectively, we provide independent evidence for our conjectures by studying the boundary condition of world-sheet under the RG-flow in GLSMs. In appendix D we find further confirmation of our results by an analysis of D-branes in the dual LG models.

5.1. Geometrical Analysis

Let us first consider the behavior of a fractional D1-brane under closed string tachyon condensation in the twisted circle theory from geometrical viewpoint. As we have explained in the previous section, a D1-brane that wraps the twisted circle once is called a fractional D1-brane. In order to understand the fate of this fractional brane under tachyon condensation, we can follow the evolution of this cycle as tachyon condensation proceeds. The geometry of the GLSM model was discussed in detail in section 3; as we argued there, the twisted circle \mathbf{S}_A^1 vanishes at $P_1 = \rho = 0$ and cannot be extended beyond this point. Indeed, near that special point this cycle is simply an angle in a 2-plane in \mathbf{R}^4 . Consequently a D1-brane wrapping the twisted cycle circle simply self annihilates at $P_1 = \rho = 0$. The induced metric on the world volume of such an annihilating brane (along one possible trajectory) is given by the everywhere smooth cigar (see Fig.4)

$$ds^2 = \frac{k}{4nP_1}(dP_1)^2 + knP_1(ds_1)^2 = (dr)^2 + n^2r^2(ds_1)^2 \quad (r \equiv \sqrt{P_1k/n}), \quad (5.1)$$

In contrast consider a bulk D1-brane. Such a brane wraps the twisted circle n times at early ‘times’, and so may be thought of as a brane wrapping the cycle \mathbf{S}_C^1 described in section 3 above. Notice that \mathbf{S}_C^1 is nontrivial in the UV ($P_1 \gg 0$) as well as in the IR. However this cycle degenerates at a point along this RG flow, and so fall in the class

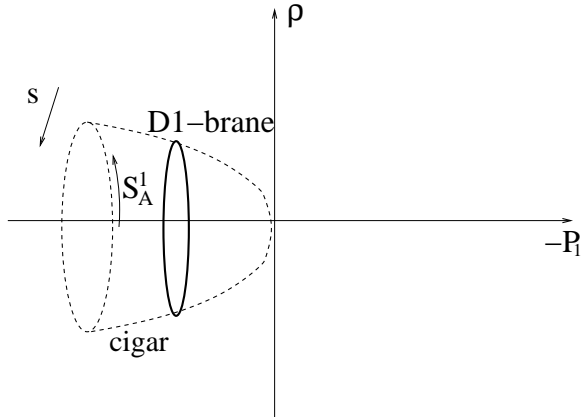


Fig. 4: The smooth cigar and wrapped D1-brane.

described in item 3. in the introduction. Correspondingly, we conjecture that a bulk 0-brane can either disappear or evolve into an ordinary brane wrapping the supersymmetric circle.¹³

On a slightly different note, observe that the supersymmetric cycle \mathbf{S}_B^1 describes the creation of a bulk zero brane (of the supersymmetric background), correspondingly we expect to find an RG flow that describes bulk 0-branes popping out of nothing.

It is also possible to extend our considerations to D3-branes. Since the world-volume for such a brane fills all of space in the UV, it will continue to do so in the IR; consequently the 3-brane of the twisted circle evolves into a usual D3-brane in flat space after the closed string tachyon condensation. As we have explained in section 4.1, twisted circle D3-branes appear in a one parameter family of solutions labeled by the Wilson line around the twisted circle. It is not difficult to trace the evolution of this Wilson line into the IR; see subsection 5.3 below.

Finally we consider the behavior of D0-branes and D2-branes in the orbifold \mathbf{C}/\mathbf{Z}_n . This is obtained by the small radius limit $R \rightarrow 0$ as we have explained¹⁴ in section 3. Thus we conclude that a fractional D0-brane will disappear after the tachyon condensation; a

¹³ Note also that \mathbf{S}_C^1 always has a non-zero radius except $P_1 = 0$. Moreover, we can slightly shift the position of \mathbf{S}_C^1 from the origin and obtain a non-contractible one cycle. In such a situation we would expect the bulk brane to survive the process of tachyon condensation.

¹⁴ We believe this limit is smooth as evidenced from e.g. the structure of GLSM [7] and the calculation of partition function [14].

bulk D0-brane either disappears or evolves into a bulk D0-brane in flat space, while a bulk D2-brane evolves into its supersymmetric counterpart (we will explain in subsection 5.3, all n \mathbf{C}/\mathbf{Z}_n D2-branes have the same end point under tachyon condensation). The latter fact for a bulk D0-brane is consistent with the results in [1]. These conclusions will be confirmed by investigating of the boundary interactions in the later subsections.

5.2. Charge Conservation

The ‘disappearance’ of a D-brane under tachyon condensation naively appears to be in conflict with charge conservation. Our geometrical description of this process makes it clear that, at least in the Euclidean version of this process, this ‘paradox’ is spurious.

As we have described above, the world volume of the ‘disappearing’ fractional D1-brane is the everywhere smooth ‘cigar’ (5.1). This Euclidean D1-brane couples to the RR-2 form field $F_{\mu\nu}$ through the everywhere conserved current

$$\sqrt{G}J^{\mu\nu} = \int d^2\sigma \frac{\partial\xi^\mu}{\partial\sigma^\alpha} \frac{\partial\xi^\nu}{\partial\sigma^\beta} \epsilon^{\alpha\beta} \prod_\lambda \delta(\xi^\lambda(\sigma) - x^\lambda); \quad (5.2)$$

certainly charge conservation is nowhere violated.

The disappearance of D-brane charge can be made to appear more puzzling upon dimensionally reducing along the twisted circle. The fractional D1-brane is charged under the gauge field obtained from the Kaluza-Klein reduction of $F_{\mu\nu}$; this charge disappears at ‘time’ $P_1 = 0$. Of course ‘charge conservation is violated’ only when the twisted circle shrinks to zero size; precisely at this point the dimensionally reduced description degenerates (for instance the 9 dimensional coupling blows up). The correct description is 10 dimensional, and manifestly charge conserving.

Of course all considerations that apply to D-strings wrapping the twisted circle also apply to ordinary strings wrapping the twisted circle. However, as we have explained behind, such strings belong to the twisted sector. Thus we conclude that twisted sector charges disappear in the process of tachyon condensation.¹⁵

¹⁵ In [13] another mechanism of the disappearance of the twisted RR-field was proposed in non-supersymmetric orbifold theories. It would be interesting to study the relation between this and our geometrical result.

Recall that the reduction of the twisted circle to the orbifold is most conveniently carried out after a T-duality; consequently, it is instructive to examine the issue of charge conservation after T-dualizing. In [24] Hori and Kapustin have demonstrated that the T-duals of gauge linear sigma models, including 2d Black hole [31] and our model defined by (3.2), lead to super potentials that break translational invariance along the dual circle. Roughly speaking, the potential may be thought of as a condensate (or plasma) of gravitons with positive and negative momentum, explaining the lack of conservation of winding or twisted strings prior to T-dualizing. It seems possible that this T-dual geometry should also be thought of as possessing a condensate of 0-branes and anti 0-branes, explaining the violation of 0-brane charge conservation.

5.3. GLSM analysis of \mathbf{C}/\mathbf{Z}_n Boundary Flows

In the previous subsections we have analyzed the evolution of the D-brane spectrum in twisted circle theories (and hence \mathbf{C}/\mathbf{Z}_n) utilizing approximate geometry for Euclidean twisted circle tachyon condensation. In this subsection we will check some of those results using more rigorous methods. Recall that twisted circle and \mathbf{C}/\mathbf{Z}_n world sheet theories are described by the UV of a GLSM (see section 3). In this section we will explicitly construct the GLSM boundary conditions that correspond to certain D-branes in these backgrounds. We then analyze the evolution of these boundary conditions under world sheet RG flow; the fate of the D-brane in question is determined by the IR limit of these boundary conditions.

The analysis of this section makes crucial use of the $\mathcal{N} = 2$ supersymmetry in the world-sheet GLSM theory. Several authors (see for instance [15][16][17][32][33][34]; see also [35] for original arguments on boundary states) have studied GLSMs on world sheets with boundaries, and determined conditions to ensure that the boundary conditions preserve $\mathcal{N} = 2$ B-type supersymmetry, and we will utilize their results below.

D2-branes

As we have reviewed above, \mathbf{C}/\mathbf{Z}_n possesses n different (fractional) 2-branes. We first consider the simplest of these 2-branes (denoted by $|0\rangle$ in section 4 above). In the

GLSM, this 2-brane corresponds to the following boundary condition [17] assuming $\theta = 0$ (see Appendix B for details of this GLSM)

$$\mathcal{D}_+\Phi = \mathcal{D}_-\Phi, \quad \Sigma = \bar{\Sigma}, \quad v_{01} = 0, \quad (5.3)$$

where Φ denotes the chiral superfields whose lowest components are ϕ_1 and ϕ_n , Σ is the twisted chiral (vector) multiplet, and v_{01} is the field strength. These boundary conditions are not modified by RG flow¹⁶.

We now turn to $|m\rangle$, the remaining $n - 1$ types of D2-branes ($m \neq 0$) in \mathbf{C}/\mathbf{Z}_n . Recall that $|m\rangle = h^m|0\rangle$ where h generates the \mathbf{Z}_n quantum symmetry of \mathbf{C}/\mathbf{Z}_n . In fact, the quantum symmetry acts very simply on the (UV of the) GLSM; it effectively shifts¹⁷ the θ angle as $\theta \rightarrow \theta + 2\pi$. This shift is an exact symmetry for a GLSM on a compact world sheet without a boundary (because $\frac{1}{2\pi} \int v$ is integrally quantized in such a theory). However its action on boundary conditions is nontrivial, (recall flux is not quantized for a 2d gauge theory on the disk). In particular in the UV of the GLSM RG flow, fractional instantons (configurations in which the phase of the vev of φ_n winds once on the boundary of the disk) violate this shift symmetry, and distinguish¹⁸ the n different D2-branes.

On shifting θ as described above the boundary condition continues to be $\mathcal{N} = 2$ supersymmetric. In fact shifts in θ are the only $\mathcal{N} = 2$ supersymmetric boundary conditions generated by marginal or relevant boundary operators (spacetime gauge fields). As the θ

¹⁶ From the sigma point of view this follows as the beta function for the spacetime gauge field vanishes when evaluated on the configuration $A_\mu = 0$. This result also follows from the Landau Ginzburg analysis, see Appendix D.

¹⁷ This fact can be easily understood in the Landau Ginzburg dual picture (see Appendix D). The shift $h : U \rightarrow U + \frac{2\pi i}{n}$ of quantum symmetry is equivalent to the shift of imaginary part of t as is obvious in eq.(D.1).

¹⁸ In fact the one point function of the bulk \mathbf{C}/\mathbf{Z}_n tachyon, on the disk, with boundary conditions corresponding to the fractional brane $|i\rangle$ is given by (see [28][36][37])

$$c_m = \mathcal{N} e^{-2\pi i m/n}. \quad (5.4)$$

This one point function corresponds to the GLSM partition function in the presence of a single fractional instanton, which is clearly proportional to $e^{-i\theta/n}$, consistent with the assignment $\theta = 2\pi m$ for the brane $|m\rangle$.

angle is not renormalized under RG flow, we conclude that the fractional branes $|m\rangle$ flow in the IR to the GLSM with Neumann boundary conditions and $\theta = 2\pi m$. However the fractional instantons that allowed one to distinguish between $|m\rangle$ in the UV are absent in the IR (because the φ_1 rather than φ_n has a vev in the IR). Consequently θ is effectively periodic with periodicity 2π in the IR, and all the n branes $|m\rangle$ evolve into the same bulk flat space D2-brane.

In order to develop intuition for these flows, we now study the evolution of the spacetime gauge fields on the m^{th} (fractional) D2-brane in the ‘classical’ sigma model approximation. As we have explained in Section 3, the world-sheet gauge field v_0 is easily computed as a function of scale in this approximation. However v_0 is simply related¹⁹ to the spacetime gauge field; $mv_0 = A_\mu(X)\partial_0 X^\mu$ [15][17]. Using these formulas we find that, for $r > 0$ (in the UV region²⁰) the flux is delta functionally localized,

$$F = -m\delta(\rho) d\rho \wedge d\theta. \quad (5.6)$$

On the other hand when $r < 0$

$$F = -\frac{2mn|r|\rho}{(n(n+1)\rho^2 + |r|)^2} d\rho \wedge d\theta. \quad (5.7)$$

Thus, as the RG-flow proceeds, the flux (5.7) (whose integral is conserved) expands out with the bubble of flat space. In the IR limit the flux is completely diluted and the n D2-branes are indistinguishable.

This property of boundary RG-flow can also be seen in the sigma model with boundary coupling $\int_{\partial\Sigma} A_\mu(X)\partial X^\mu$. The one loop RG-flow equation [38] leads to (in the weak curvature approximation)

$$\frac{\partial A_\mu}{\partial\lambda} = \nabla^\nu F_{\nu\mu} - \xi^\nu F_{\mu\nu} + \nabla^\nu \phi F_{\mu\nu}, \quad (5.8)$$

¹⁹ This is shown by the identification of the boundary coupling

$$m \int dx^0 \left(\frac{\sigma + \bar{\sigma}}{2} - v_0 \right), \quad (5.5)$$

with the usual sigma model gauge coupling $\int A^\mu(X)\partial_0 X^\mu$ setting $\sigma = 0$ in the Higgs branch. This gauge coupling comes from the shift of the parameter θ in the term $\frac{\theta}{2\pi} \int v$. The σ dependent term is also induced to preserve $\mathcal{N} = 2$ supersymmetry (see [17]).

²⁰ Under the RG-flow the FI parameter r changes following (B.2) as reviewed in the Appendix B. The UV limit corresponds to $r = \infty$, while IR limit to $r = -\infty$.

where λ is the logarithm of length scale (proportional to $|r|$ in (5.7)) under the flow and ξ^ν represents the freedom of coordinate transformations. After we substitute the results²¹ of bulk RG-flow in [18], we obtain the following equation assuming that only A_θ is nonzero,

$$\frac{\partial A_\theta}{\partial \lambda} = \frac{s}{f(s)\lambda} \partial_s \left(\frac{1}{f(s)s} \partial_s A_\theta + \frac{1}{2} A_\theta \right), \quad (5.9)$$

where we rescaled the coordinate as $s = \rho/\sqrt{\lambda}$ and defined the function $f(s)$ by $f(s) = (1 + W(\frac{1}{n} - 1 - s^2/2))^{-1}$ (W is the inverse function of xe^x). By setting the right-hand side of (5.9) to zero, we find a solution (up to constant shift)

$$A_\theta = A_\theta(0) \cdot e^{-\int_0^s \frac{s' f(s')}{2} ds'}. \quad (5.10)$$

After transforming into the previous radial coordinate ρ we get the gauge flux

$$F_{\rho\theta} = -\frac{A_\theta(0) \cdot f(\rho/\sqrt{\lambda}) \cdot \rho/\sqrt{\lambda}}{2\sqrt{\lambda}} \cdot e^{-\int_0^{\rho/\sqrt{\lambda}} \frac{s' f(s')}{2} ds'}. \quad (5.11)$$

Since the function f satisfies the bound $1/n < f < 1$, it is obvious that the flux $F_{\rho\theta}$ value takes its the maximum at $\rho \sim O(\sqrt{\lambda})$ as in (5.7) and the asymptotic behavior ($r \rightarrow \infty$) is similar to the solution to diffusion equation as $F_{\rho\theta} \sim e^{-\frac{f\rho^2}{4\lambda}}$. Thus it is completely smeared in the IR limit $\lambda \rightarrow \infty$ and we again confirmed the diffusion property in a different picture.

It is instructive to analyze how the spectrum of open strings between the fractional branes $|0\rangle$ and $|m\rangle$ evolves as a function of RG scale. In the UV the relative (spacetime) field strength between these two branes is given by (5.6) (or equally, a Wilson line

$$\int_0^{\frac{2\pi}{n}} A_\theta d\theta = -\frac{2\pi m}{n}, \quad (5.12)$$

in the ‘angle’ direction). Consequently, open strings stretching between these branes obey twisted boundary conditions. For instance the (open string) tachyon field obeys

$$T(z) = e^{-2\pi im/n} T(gz), \quad (5.13)$$

²¹ They are given by the metric $(ds)^2 = \lambda(f(s)^2 ds^2 + s^2 d\theta^2)$ and the parameter $\xi = \frac{1}{2} s f(s) ds$ with zero dilaton [18].

where the operator g acts on the coordinate z of \mathbf{C}/\mathbf{Z}_n as $g : z \rightarrow e^{2\pi i/n} z$ in agreement with (4.1). As the RG flow proceeds towards the IR, however, the flux enclosed within a circle of any finite spacetime radius (and hence the effective Wilson line at that radius) goes to zero (see (5.7)). In other words the world-volume fields obey twisted boundary condition like (5.13) for $|z| \gg \sqrt{|r|}$, but satisfy the untwisted one inside the bubble of flat space $|z| \ll \sqrt{|r|}$.

D0-branes

We will now study the evolution of D0-brane boundary conditions under the RG flow. Unfortunately it appears difficult to find simple boundary conditions that both preserve $\mathcal{N} = 2$ and also reduce in the UV to the D0-brane; however, we can circumvent this problem with a trick. As we will explain below, it is straightforward to construct $\mathcal{N} = 2$ GLSM boundary conditions that reduce in the UV to the $D2 - \bar{D}2$ system. These boundary conditions may then be deformed (while preserving $\mathcal{N} = 2$ supersymmetry) by turning on a vortex for the open string tachyon. The resulting boundary condition may be interpreted as a single D0-brane (the $D2 - \bar{D}2$ brane have disappeared via open string tachyon condensation [39]). Non renormalization of the boundary super potential (guaranteed by $\mathcal{N} = 2$ supersymmetry) allows us to follow the evolution of the boundary conditions as a function of RG scale, and determine the fate of fractional D0-branes under tachyon condensation.

To be more concrete, let us consider the $D2\bar{D}2$ system in \mathbf{C}/\mathbf{Z}_n where the $D2$ brane is of type $|0\rangle$ and the $\bar{D}2$ brane is of type $|m\rangle$ from the viewpoint of GLSM. As we have seen before, the action of \mathbf{Z}_n quantum symmetry (or equally the shift of θ by 2π) changes the types of 2-branes in UV limit. Since the shift of θ by $2\pi n$ is the symmetry of GLSM with boundary in the orbifold limit, we have the periodicity $|m+n\rangle = |m\rangle$ at the beginning of the RG-flow.

In order to construct boundary conditions that represent the $D2 - \bar{D}2$ system, we must introduce Chan Paton factors. This is conveniently achieved by introducing a new complex fermionic boundary variable η . It will turn out (see below) that η and its conjugate $\bar{\eta}$ obey the conjugation relations $\{\eta, \bar{\eta}\} = 1$; consequently quantization leads to a two state

system. Operators on this Hilbert space are 2×2 matrices; as expected for the $D2\bar{D}2$ system.

Then the $D2\bar{D}2$ system in \mathbf{C}/\mathbf{Z}_n is described by the GLSM with boundary conditions (5.3), together with gauge invariant boundary interactions (this can also be seen as the boundary string field theory [40][41] for brane-antibrane system [42])

$$S_{\partial\Sigma} = \int_{\partial\Sigma} d\tau d\theta d\bar{\theta} \bar{\Gamma} e^{-mV} \Gamma + \int_{\partial\Sigma} d\tau d\theta \Gamma T(\Phi) + (h.c.), \quad (5.14)$$

where Γ is a charge m boundary fermionic chiral superfield²² whose lowest component is η

$$\Gamma = \eta + \theta F - i\theta\bar{\theta}\partial_\tau\eta, \quad (5.15)$$

and V is the GLSM vector superfield whose lowest component is given by $(v_0 - \frac{\sigma + \bar{\sigma}}{2})\theta\bar{\theta}$.

In components, the first term in (5.14) is simply

$$-m \int \bar{\eta}\eta(v_0 - \frac{\sigma + \bar{\sigma}}{2}) \sim -m \int \frac{\sigma_3}{2}(v_0 - \frac{\sigma + \bar{\sigma}}{2}), \quad (5.16)$$

the analogue of (5.5) on a single D2-brane. Note, in particular, that $v_0 = \partial_\tau X^\mu A_\mu(X)$ ²³ where A_μ is the relative gauge field in the $D2\bar{D}2$ system. The second term in (5.14) represents the boundary deformations corresponding to the open-string tachyon field $T(\Phi)$, where T is a complex scalar.

It turns out that the GLSM with boundary conditions (5.3) and boundary interactions (5.14) preserves $\mathcal{N} = 2$ supersymmetry provided that the tachyon T is a holomorphic function of Φ . The simplest solution to this condition is $T = 0$; this represents a $D2 - \bar{D}2$ system in the UV, and flows to a usual $D2 - \bar{D}2$ system in the IR. In particular, the open string tachyon, which is protected against quantum corrections owing to a non-renormalization theorem, remains zero throughout the flow.

²² In the UV limit this charge means that the \mathbf{Z}_n orbifold action acts as $\Gamma \rightarrow \Gamma e^{2\pi i/m}$. Thus the tachyon followed the projection $T \rightarrow T e^{-2\pi i/m}$. This fact agrees with (5.13).

²³ The scalar field σ , which is in the same $\mathcal{N} = 2$ multiplet as v_μ , is taken to be zero since we are interested in the Higgs branch. For the analysis of the Coulomb branch in similar GLSMs see [13].

Flows from bulk 0-branes into bulk 0-branes

We now consider boundary conditions with the open string tachyon turned on. We first consider the case $m = 0$ (i.e. the 2-brane and anti 2-brane are of the same variety). In this situation Γ is uncharged; consequently gauge invariance of (5.14) requires that $T(\Phi)$ should be gauge invariant (uncharged). The simplest example is given as follows

$$T(\Phi_{-n}, \Phi_1) = T_1 \Phi_{-n} (\Phi_1)^n, \quad (5.17)$$

where the coefficient T_1 corresponds to the strength of the open-string tachyon field. In the UV limit the field Φ_{-n} has a large expectation value and can be replaced by \sqrt{r}/n , while Φ_1 can be regarded as a coordinate of the orbifold \mathbf{C}/\mathbf{Z}_n . Thus the tachyon field is expressed²⁴

$$T(z) = \frac{T_1 \sqrt{r}}{n} z^n. \quad (5.18)$$

In the deep UV $T(z) = kz^n$ where k diverges; and so represents a bulk D0-brane [43] at the origin of the orbifold. (The tachyon field (5.17) has winding number n and so would have represented n D0-branes in flat space. A bulk 0-brane on \mathbf{C}/\mathbf{Z}_n is precisely a collection of n covering space 0-branes modded out by the projection, explaining our identification).

On the other hand, in the IR limit, the field ϕ_1 has an expectation value $\phi_1 \approx \sqrt{|r|}$, and another field ϕ_n is identified with z the coordinate in flat space. The tachyon field configuration (5.17)

$$T(z) = T_1 \sqrt{|r|} z, \quad (5.19)$$

has unit winding number and so may be identified with a D0-brane in the flat space. Thus we conclude that a bulk D0-brane evolves into an ordinary D0-brane the closed string tachyon condensation, consistent with the results of subsection 5.1.

This analysis is easily extended to more complicated tachyon configurations. By following the RG flow in the presence of the polynomial valued tachyon field

$$T(\Phi_{-n}, \Phi_1) = \sum_{l=0} T_l (\Phi_{-n} (\Phi_1)^n)^l, \quad (5.20)$$

²⁴ Note that this field configuration satisfies the projection (5.13) setting $m = 0$.

we conclude that a configuration of n separated bulk D0-branes (located at the zeros of $\sum_{l=0} T_l w^l = 0$) evolve into n separated D0 branes in flat space.

Flows from bulk 0-branes into nothing

We can also choose the following tachyon field for the same kind of $D2 - \bar{D}2$ system setting $m = n$ (remember the periodicity $|m + n\rangle = |m\rangle$ in the UV limit)

$$T(\Phi_{-n}, \Phi_1) = T_1(\Phi_1)^n. \quad (5.21)$$

Even though the starting point is the same as before (a bulk D0-brane), the final product is different. Since the tachyon field takes a large constant value and is completely condensed in the end, the bulk D0-brane disappears in this process. Note also that this only happens near the origin ($z = 0$) because it is impossible to shift the location of the D0-brane away from the origin as in (5.20). These results are completely consistent with those obtained from the geometrical consideration in section 5.1.

Flows from fractional 0-branes into nothing

We now turn to the study of tachyon condensation on the more general system consisting of a D2-brane $|m\rangle_{D2}$ and an anti D2-brane $|\bar{0}\rangle_{D2}$. In this situation Γ has charge $-m$, and charge conservation demands that $T(\varphi)$ have charge m . The simplest example of such a tachyon field is

$$T(\Phi_{-n}, \Phi_1) = T_1(\Phi_1)^m. \quad (5.22)$$

In the UV the tachyon field $T(z) \sim z^m$ may be interpreted as representing $|m\rangle_{D0}, |m - 1\rangle_{D0}, \dots, |1\rangle_{D0}$ (this follows from an analysis of the RR charges of this configuration, see [43]). On the other hand, in the IR limit $\phi_1 \approx \sqrt{|r|}$ and the tachyon field is simply constant (and this constant value increases without bound as we flow to the deep IR). Thus the open string tachyon is completely condensed; all open string degrees of freedom vanish in this limit; consequently the fractional 0-brane has simply disappeared. This matches the results of section 5.1 again.

0-brane production from nothing

Finally, let us consider the case of $m = -n$ (the same kind of D2 and antiD2). Then an allowed tachyon field is

$$T(\Phi_{-n}, \Phi_1) = T_1 \Phi_{-n}, \quad (5.23)$$

which shows the initial nothing state will become a D0-brane in the flat space after the closed string tachyon condensation. Once again, this also matches with the previous geometrical argument and corresponds to the cycle \mathbf{S}_B^1 .

5.4. GLSM Analysis of Twisted Circle Boundary Flows

As we have described in section 3, the decay of twisted circle theories via closed string tachyon condensation could easily be understood utilizing a GLSM. The low energy limit of the GLSM is a CFT with a Liouville factor; the Liouville direction may (roughly) be thought of as a scale or Euclidean time. In this subsection we will study the same GLSM on a world sheet with a boundary, imposing boundary conditions that preserve $\mathcal{N} = 2$ B-type world sheet supersymmetry. The boundary conditions we study will always be Neumann in the Liouville (P_1) direction (this is required for $\mathcal{N} = 2$ world sheet supersymmetry, [44][45]); and in most examples we study the boundary interaction will also be independent of P_1 . As in the previous subsection, $\mathcal{N} = 2$ supersymmetry guarantees these features persist in the low energy CFT; it is then a simple matter to follow the boundary conditions, and hence trace the D-branes from $P_1 \gg 0$ (twisted circle) to $P_1 \ll 0$ (supersymmetric circle). As the arguments of this subsection closely mimic those of the previous subsection, we will be very brief.

The decay of a twisted circle D3-brane is described by a D4-brane in the GLSM of section 3. The twisted circle D3-brane with zero Wilson line is described by Neumann boundary conditions on $\varphi_1, \varphi_n, P_1$ and P_2 , together with the conditions $v_1 = v_{01} = 0$ on the boundary (these conditions preserve $\mathcal{N} = 2$ B-type world sheet supersymmetry). Turning on a Wilson line corresponds to adding the boundary interaction (5.5). The UV Wilson line $\frac{2\pi m}{n}$ (m in (5.5) varies continuously between 0 and n) evolves into²⁵ the IR Wilson line $2\pi m$.

²⁵ Taking the zero radius limit (see subsection 4.2) we conclude that all \mathbf{C}/\mathbf{Z}_n fractional 2-branes map into the bulk flat space 2-brane, in agreement with the previous subsection.

As in the previous subsection, it is possible to construct the twisted circle fractional D1 brane (D2 brane on including the Liouville direction) via $D3\bar{D}3$ ($D4\bar{D}4$ on including the Liouville direction) tachyon condensation. P_1 independent boundary deformations of the $D4\bar{D}4$ are identical to (5.17) for a bulk D-brane and (5.22) for a fractional D-brane. The arguments and conclusions of the previous subsection carry through almost unmodified, once again confirming the geometrical reasoning of subsection 5.1. In particular, we find that the bulk D1-brane in the twisted circle either disappears or evolves into an ordinary D1-brane in flat space after the closed string tachyon condensation. On the other hand, the fractional D1-brane disappears from the spectrum.

Finally we should point out that it is also possible to construct large classes of $\mathcal{N} = 2$ boundary interactions which depend on P . For example, we can take

$$T(P, \Phi_{-n}, \Phi_1) = T_1(\Phi_1)^{m+q} e^{-qP}. \quad (5.24)$$

These are expected to lead to other boundary states of the GLSM after the boundary RG-flow²⁶. We will not investigate the relevance of these D-branes to our closed string tachyon condensation.

6. Evolution of D-branes under More General RG Flows

Before we conclude this paper, we would like to apply our method of analyzing D-brane spectrum to more general RG flows. In particular, let us consider²⁷ the RG Flows from $(\mathbf{C} \times \mathbf{S}^1)/\mathbf{Z}_n$ to $(\mathbf{C} \times \mathbf{S}^1)/\mathbf{Z}_m$ ($n > m$). We further assume that n and m are coprime. Then we can construct gauged linear sigma models which describe these RG-flows in the same way as before. This is defined by just replacing the chiral superfields Φ_1 in (3.2) with the charge m superfields Φ_m in the model discussed in section 3.1. If we take the small radius limit $k \rightarrow 0$, then it reduces to the RG-flow from \mathbf{C}/\mathbf{Z}_n to \mathbf{C}/\mathbf{Z}_m , which is also realized as a gauged linear sigma model in the same way [3].

²⁶ Here we should consider relevant perturbations $q < \frac{k}{4(n-1)}$ or marginal one $q = \frac{k}{4(n-1)}$.

²⁷ We are very grateful to A. Adams and R. Gopakumar for suggesting an investigation of this case to us.

Now let us consider the evolution of D-branes under these RG-flows²⁸. For simplicity, we consider the explicit example of $(n, m) = (5, 3)$, though its generalization is obviously straightforward. Again we can apply two different methods.

First, we analyze the geometrical picture as in section 5.1. We can compute the classical metric as in Appendix C and indeed get smooth four geometry. In the UV limit it approaches the metric of $(\mathbf{C} \times \mathbf{S}^1)/\mathbf{Z}_n$ given by (3.5), while in the IR limit it becomes the metric of $(\mathbf{C} \times \mathbf{S}^1)/\mathbf{Z}_m$

$$ds^2 = d\rho'^2 + \frac{n^2}{m^2} \rho'^2 d\theta^2 + \frac{k}{2} \left(\frac{d\theta}{m} - dP_2 \right)^2. \quad (6.1)$$

Note that the angle $\theta (\equiv \theta_m)$ has the periodicity 2π and also we have the \mathbf{Z}_n identification $(\theta, P_2) \sim (\theta + \frac{2\pi m}{n}, P_2 + \frac{2\pi}{n})$.

Consider a fractional D1-brane wrapped on the twisted circle \mathbf{S}_A^1 in the UV defined in the same way as in section 3.3 (see Fig.5). After the RG flow, it again disappears as we can see from (6.1) explicitly. However, a bound state of two fractional D1-branes wraps a cycle equivalent to \mathbf{S}_D^1 (equivalence upto the shift of the UV trivial cycle \mathbf{S}_B^1). It follows from (6.1) that the cycle \mathbf{S}_D^1 degenerates at $\rho' = 0$, but then evolves into the twisted circle of $(\mathbf{C} \times \mathbf{S}^1)/\mathbf{Z}_m$ upon subsequent evolution. Thus we predict that even though a single fractional D1-brane disappears under tachyon condensation, a bound state of two such branes can either evolve into a fractional D1-brane or disappear upon closed tachyon condensation. On the other hand, if we consider a bulk D1-brane wrapped on \mathbf{S}_C^1 , it will simply evolve into a bulk D1-brane in the IR twisted circle as in the previous case of $m = 1$.

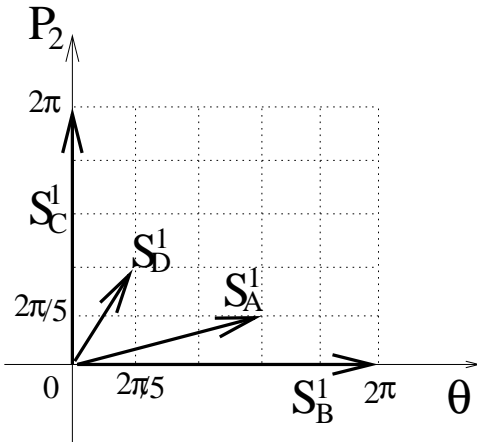


Fig. 5: Various cycles in the twisted circle $(\mathbf{C} \times \mathbf{S}^1)/\mathbf{Z}_5$.

²⁸ Even though we use the terminology of D-branes in the twisted circle theory, we can also get the equivalent result for the D-branes in the orbifold.

Next let us understand the above result by employing the analysis of $\mathcal{N} = 2$ supersymmetric boundary interaction. The tachyon configurations

$$T = T_1\Phi_3, \quad T_1(\Phi_3)^2, \quad T_1(\Phi_3)^2\Phi_{-5}, \quad T_1(\Phi_3)^5(\Phi_{-5})^3, \quad T_1(\Phi_3)^5, \quad T_1(\Phi_{-5})^3, \quad (6.2)$$

respectively represent

1. The disappearance of a single fractional D0-brane.
2. The disappearance of the bound state of two fractional D0-branes.
3. The evolution of a bound state of 2 fractional D0-branes into a single fractional D0-brane.
4. The evolution of a bulk D0-brane into a bulk D0-brane.
5. The disappearance of a bulk D0-brane.
6. The creation of a bulk D0-brane out of nothing.

Note the striking match between geometrically inspired conjectures and our explicit constructions of boundary RG flows. Indeed, the tachyon fields (6.2) explicitly encode the information of the lattice vectors (see Fig.5) via the ‘translation rule’ $\Phi_m \leftrightarrow \mathbf{S}_A^1$ and $\Phi_{-n} \leftrightarrow -\mathbf{S}_B^1$. This obviously allows us to see the results of D-brane evolutions under the general (n, m) RG flow²⁹.

7. Discussion

In this paper we have studied the evolution of D-branes under closed string tachyon condensation in non-supersymmetric orbifold and twisted circle backgrounds. Our analysis employed two complementary methods. First, we used the gauge linear model description of the twisted circle tachyon condensation process to derive a smooth four dimensional geometry that approximately describes the evolution of the twisted circle in an energy scale (roughly Euclidean time) direction. Interpreting the branes of the twisted circle theory as usual type II branes wrapping nontrivial cycles, we traced the evolution of these

²⁹ The evolution of D3-branes can also be discussed in the GLSM picture. A D3-brane is parametrized by the Wilson line $\frac{2\pi l}{n}$ ($0 \leq l < n$) in the UV limit. After the RG flow, the periodicity becomes small as $0 \leq l < m$ by the radius change.

cycles as the tachyon condensed. Our second method involved the analysis of RG flows in gauged linear sigma models on the disk; we used world sheet $\mathcal{N} = 2$ supersymmetry to follow the evolution of boundary interactions (sometimes using ideas from boundary string field theory) into the IR. Both methods yielded the same result; localized D-branes disappear (or evolve other fractional D-branes in general RG flows) as the closed string tachyon condenses, while D-branes that are not tied to the fixed point either disappear or evolve into usual D-branes in flat space.

Our study suggests several directions for future study. First, twisted circle tachyon condensation is only approximately described by the four dimensional Euclidean geometry studied in this paper. The exact process is captured by flowing the sigma model based on this approximate geometry to the IR. It would be intensely interesting to find an exact description of the resultant $\mathcal{N} = 2$ CFT. Indeed Hori and Kapustin [24] were able to solve a related problem in the simpler setting of 2d Black hole. Such a description would permit detailed understandings of several aspects of the process of tachyon condensation.

Secondly, we have only studied tachyon condensation as a function of the Liouville direction (roughly Euclidean time). It is certainly important to understand the Lorentzian analogue of this process (the evolution of this background as a function of time). It is not clear to us that the Euclidean and Lorentzian processes are even qualitatively similar; for instance the geometry on equal ‘time’ (P_1) cycles of our smooth 4-geometry (3.7) degenerates at the slice $P_1 = 0$. It would be very interesting to understand this issue better³⁰.

Our second approach to this problem also highlights several interesting connections. As we have explained the world sheet RG flow with certain boundary conditions (for instance boundary conditions corresponding to the fractional 0-brane of \mathbf{C}/\mathbf{Z}_n) leads to world sheet theory with no boundary in the IR. As we have explained in subsection 5.3, there is a sense in which closed string tachyon condensation triggers open string tachyon condensation on an initially stable brane. Intuitively, it is not difficult to understand why this happens. For instance, the fractional 0-brane of \mathbf{C}/\mathbf{Z}_n may be ‘blown up’ into a

³⁰ See [18] for a recent discussion on the connection between world sheet RG flow and time evolution.

D1-brane wrapping a twisted circle. This circle (non contractible in the UV) degenerates in the process of the closed string tachyon condensation. The degeneration of this cycle allows the $D1$ brane circular loop to self annihilate via open string tachyon condensation (analogous to $D1\bar{D}1$ annihilation). As is remarkable even in the general RG flow analysis in section 6, we can obtain the same conclusions from our two different viewpoints. This might be mathematically regarded as a novel correspondence (analogous to McKay correspondence³¹) between geometrical structure and algebraic one under ‘time’ evolution.

Another interesting direction of investigation concerns the limit $n \rightarrow \infty$ of the models studied in this paper. As we have explained in Section 2, in this limit the twisted circle reduces to an orbifold of type 0 theory. If the study of tachyon condensation commutes with $n \rightarrow \infty$, the results of this paper determine the fate of several type 0 D-branes under the process of closed string tachyon condensation. As the type 0 tachyon is delocalized, type 0 tachyon condensation is particularly interesting, and deserves further study.

Finally, in this paper we have considered configurations consisting of a fixed number of D-branes, in the classical limit $g_{string} \rightarrow 0$. In this limit D-branes probe (and react to) the closed string geometry, but do not back react on it. New interesting phenomena may occur in other limits; for instance if the number of branes is taken to infinity. We leave such investigations to future work.

Acknowledgments

We would like to thank J. David, T. Eguchi, M. Gutperle, Y.Hikida, A. Iqbal, T. Kawano, Y. Michishita, A. Sen, E. Silverstein, A. Strominger, H. Takayanagi, D. Tong, N. Toumbas, C. Vafa, S. Yamaguchi, P. Yi and especially A. Adams, R. Gopakumar, M. Headrick and K. Hori for several extremely useful discussions. We would particularly like to thank M. Headrick for disabusing us of a potentially embarrassing misconception. The work of SM was supported in part by DOE grant DE-FG03-91ER40654 and a Harvard Junior Fellowship. The work of TT was supported in part by DOE grant DE-FG03-91ER40654.

³¹ See also [13][46] for similar discussions in four dimensional unstable orbifolds.

Appendix A. Type 0 theory and Interpolating Orbifolds

Type 0A/B theory may be regarded as an orbifold by $(-1)^{F_s}$ (F_s is the spacetime fermion number) of type IIA/B theory. This is most easily seen at the level of the torus partition function. The projection by $(-1)^{F_s}$ retains only states in the NS-NS or RR sectors of the theory, i.e. states with fermion boundary conditions $(-, -)$ or $(+, +)$ on the σ cycle of the torus. It now remains to add in the twisted sectors; as the net result of this process is symmetric (i.e. modular invariant) between the two cycles of the torus, the final partition function thus contains only $(+, +)$ and $(-, -)$ along the τ cycle as well and the resulting partition function is that of type 0A/B.

Recall, that type 0A and type 0B theory are T-dual to each other; under T-duality $\psi_9 \rightarrow -\psi_9$, and so $(-1)^{F_l+F_r} \rightarrow -(-1)^{F_l+F_r}$ in the Ramond sector (this is most clearly seen on expressing $(-1)^{F_l+F_r}$ in terms of bosonized fermions), interchanging type 0A and type 0B.

We now move onto the consideration of a slightly more involved orbifold of type IIA/B theory; the orbifold by $(-1)^{F_s} \times \sigma$ where σ represents a shift by $2\pi R$ in the z direction [22]. As we now review, in the $R \rightarrow 0$ limit this so called ‘interpolating orbifold’ is equivalent to type 0B theory on \mathbf{R}^{10} ; it interpolates between IIA theory on \mathbf{R}^{10} (as $R \rightarrow \infty$) and 0B theory on \mathbf{R}^{10} (as $R \rightarrow 0$). It is clear that the projection by $(-1)^{F_s} \times \sigma$ retains only fermions of half odd momentum and bosons of integral momentum around the z circle. At the level of the torus partition function, the sum over windings of the τ cycle over the spacetime circle (parameterized by the winding number w_τ) is weighted by the additional factor $(-1)^{w_t}$ in the $(-, +)$ or $(+, -)$ sectors. Once again, the symmetry of the twisting procedure between the σ and the τ cycles demands that the summation over windings in the σ direction be weighted by $(-1)^{w_s}$ when the fermions have $(-, +)$ or $(+, -)$ boundary conditions in the τ direction. This reverses the GSO projection, setting $(-1)^{F_L} = (-1)^{F_R} = 1$, (instead of the usual $(-1)^{F_L} = (-1)^{F_R} = -1$) in sectors of odd winding.

In summary, this orbifold retains only fermions of half odd momentum and bosons of integral momentum. Furthermore, the GSO projection is reversed in sectors of odd winding. It is now clear that the orbifold of IIA theory by $(-1)^{F_s} \times \sigma$ reduces, as $R \rightarrow 0$,

to 0B theory in noncompact \mathbf{R}^{10} . In this limit all the states of non-zero momentum around the circle are lifted out of the spectrum and this includes all the fermions (since by the antiperiodic boundary conditions they have half-integral momenta). In the sector with zero-momentum along the circle, the only effect of the boundary conditions is to reverse the GSO projection for states of odd winding number w . Thus when $w = 2w'$ (w is the winding number) the spectrum consists of the (NS+,NS+) and (R+,R-) sectors, and for $w = 2w' + 1$ the (NS-,NS-) and (R-,R+) sectors. This is approximately the spectrum in the zero-momentum, winding number w' sector of type 0A theory on a circle of radius $2R$. This equality becomes exact in the limit $R \rightarrow 0$, where it is more appropriate to describe the theory as 0B in infinite flat space.

We now describe the T-dual of the interpolating orbifold. T-duality is easiest to understand in terms of states rather than partition functions. As usual, T-duality interchanges momentum and winding. The T-dual theory is most usefully thought of as a theory with radius $\frac{\alpha'}{2R}$. Sectors of odd winding are all fermions, sectors of even winding are all bosons. In addition, states of integral momentum have the IIB/A GSO projection, while states of half odd momentum have the reversed GSO projection. In the limit that $R \rightarrow 0$, this theory is approximately type 0B/A theory on a circle of radius $\frac{\alpha'}{2R}$. At finite R the model is an orbifold of type 0B/A theory by $(-1)^{F_L} \times \sigma'$ where σ' is a shift by $\frac{2\pi\alpha'}{2R}$ in the z direction. The projection associated with this orbifold ensures that states with the usual (IIB) GSO projection have integral momentum; states with the opposite GSO projection have half odd momentum. Twisted sectors then produce the rest of the spectrum, as may be seen, as usual, by demanding symmetry of the partition function under $\sigma \leftrightarrow \tau$.

Appendix B. Decay of \mathbf{C}/\mathbf{Z}_n

B.1. Review of Tachyon Condensation in \mathbf{C}/\mathbf{Z}_n

Recall that type II theory on \mathbf{C}/\mathbf{Z}_n has tachyons in its twisted sectors. Adams Polchinski and Silverstein (APS) argued that the tachyon condensation process in this background nucleates a bubble of flat space at the tip of the cone [1]; the bubble then grows without bound.

Let us consider the actual process of tachyon condensation in more detail. Let the initial state of the system be given by the \mathbf{C}/\mathbf{Z}_n background perturbed by $\int d^2z \epsilon T$ (in 0-picture), where T is the most relevant twisted sector operator. The subsequent evolution of the system under worldsheet RG flow has two distinct stages. The first stage (the stage of linear growth) is characterized by the condition $\epsilon \ll 1$. In this stage ϵ simply grows with RG scale at a rate determined by the $2(1 - \delta)$, where δ is the holomorphic scaling dimension of T ; no other operators are turned on. Eventually ϵ grows to unit order, and begins to mix in a nonlinear fashion with all other operators. At this point the spacetime metric (hence target space geometry) begins to evolve with RG scale, and we enter the second stage of the RG flow. According to the APS conjecture, in this stage a large bubble of flat two dimensional space is nucleated about the tip of (what was) the \mathbf{C}/\mathbf{Z}_n cone, and this bubble then grows without bound. Once the size of the bubble is large in string unit, the further evolution of the system is accurately described by the 1-loop RG equations of the worldsheet nonlinear sigma model.

In order to substantiate this picture, APS first computed the metric on the moduli space of D0-branes in the \mathbf{C}/\mathbf{Z}_n background perturbed by $\int d^2z \epsilon T$, where $\epsilon \ll 1$. They found that the 0-brane moduli space is \mathbf{C}/\mathbf{Z}_n with the singularity smoothed out at length scale $\epsilon\sqrt{\alpha'}$. This demonstrates that D-branes already see the first stage of the RG flow in terms of a growing bubble of flat space. Once the size of this bubble becomes large in string units, a fundamental string must see the same geometry as the D0-brane; consequently this computation provides evidence for the conjecture described above. In order to further substantiate their picture, APS went on to find an approximate solution³² to the 1-loop worldsheet RG equations on the string worldsheet (valid once the flat space bubble is large in string units) corresponding to this bubble steadily expanding in a sea of \mathbf{C}/\mathbf{Z}_n .

In summary, according to the APS picture, D-branes see the tachyon condensation³³ process as an always expanding bubble of flat space. Closed strings see a two stage process.

³² An exact solution with the same property was later found in [18].

³³ Most recent studies of the subject utilize worldsheet RG flow (or Liouville flow) to study tachyon condensation. A recent discussion of the connection between world sheet RG flow and the physically more interesting time evolution, may be found in [18].

In the first stage, the tachyon grows but all other operators including the metric are unaffected, and (geometrically speaking) nothing happens. Eventually, however, (when the coefficient of the tachyon is of order unity, which is also when the D-brane bubble becomes string scale) the tachyon backreacts onto the geometry, producing a string scale bubble of flat space, which then proceeds to grow in a diffusive fashion.

Following up on the work of APS, Vafa [3] presented an exact construction of the RG flow on the string worldsheet by examining the low energy behavior of a particular gauged linear sigma model. We will review this construction below.

B.2. Tachyon Condensation using the Gauged Linear Sigma Model Construction

In this subsection we review Vafa's construction of the RG flow describing \mathbf{C}/\mathbf{Z}_n decay utilizing a two dimensional $\mathcal{N} = (2, 2)$ $U(1)$ gauge theory (so called gauged linear sigma model (GLSM) [23]).

Consider a gauge linear sigma model with action

$$S = \frac{1}{2\pi} \int d^2\sigma \left[d^4\theta \left(\bar{\Phi}_1 e^V \Phi_1 + \bar{\Phi}_{-n} e^{-nV} \Phi_{-n} - \frac{1}{2e^2} |\Sigma|^2 \right) + \text{Re} \int d^2\tilde{\theta} t \Sigma \right], \quad (\text{B.1})$$

where the two charged chiral superfields Φ_1 and Φ_{-n} transform under $U(1)$ gauge transformations as in (3.2), V represents a vector multiplet and its lowest component is a gauge field v_μ (its field strength is defined to be v_{01}); the twisted chiral superfield Σ is its superfield-strength. The complex valued constant³⁴ $t = r + i\theta$ parameterizes both the Fayet-Iliopoulos term $r \int d^4\theta V$ and the theta term $\frac{\theta}{2\pi} \int v_{01}$.

The quantum theory generated by (B.1) is super renormalizable; in fact it is easy to verify that all correlators are rendered finite after a simple one loop renormalization of the FI term (see section 3, [23])

$$r_0(\Lambda_0) = r(\Lambda) + (n - 1) \ln\left(\frac{\Lambda_0}{\Lambda}\right). \quad (\text{B.2})$$

Here r_0 is the bare FI term defined at the cut off scale Λ_0 , and r is the finite FI term associated with the finite renormalization scale Λ .

³⁴ Actually r is renormalized and runs as a function of energy scale as we will see later.

B.3. The Sigma Model Limit

Consider the low energy dynamics of (B.1). In Wess-Zumino gauge, the terms involving the auxiliary gauge field D are

$$\frac{1}{2\pi} \int d^2\sigma \left(\frac{D^2}{2e^2} + D(|\varphi_1|^2 - n|\varphi_{-n}|^2 + r) \right), \quad (\text{B.3})$$

where φ_1, φ_{-n} are the lowest components of Φ_1, Φ_{-n} respectively. At energies small compared to e we may restrict attention to fluctuations on the supersymmetric manifold of zero-energy configurations satisfying

$$-\frac{D}{e^2} = |\varphi_1|^2 - n|\varphi_{-n}|^2 + r = 0. \quad (\text{B.4})$$

The moduli space of classical vacua is parameterized by φ_1 and φ_{-n} constrained according to (B.4) modulo gauge transformations, so that the dynamics is that of a one complex dimensional supersymmetric sigma model.

B.4. GSO Projection

We have described above how the GLSM reduces at low energies, to a sigma model. We will now describe an exact \mathbf{Z}_2 symmetry of the GLSM that flows at low energies to $(-1)^{F_L}$ on the sigma model (similar remarks apply to $(-1)^{F_R}$). This symmetry may then be used to impose a type II ‘GSO projection’ on the GLSM.

Classically, the gauge theory has a discrete chiral symmetry given by $\psi_- \rightarrow -\psi_-$, $v_\mu \rightarrow -v_\mu$, $\lambda_+ \rightarrow -\lambda_+$ (all other fields are invariant; v_μ and λ are the gauge boson and the spinor respectively in the gauge multiplet, and ψ_- represent the negative chirality components of all matter fermions - this a special example of the left moving R symmetry described, for instance, in section 2 of [23].) is a symmetry of the gauge theory Lagrangian; we call the operator that generates this symmetry $(-1)^{F_L}$. This change of variables induces a Jacobian $(-1)^{\frac{n-1}{2\pi}} \int v_{01}$ in the quantum path integral; this Jacobian is trivial if and only if n is odd. Thus $(-1)^{F_L}$ is non-anomalous in the quantum theory if n is odd, as we assume in this paper.

B.5. The Sigma Model in the UV

Let us start with the UV limit $r = \infty$. We can use the gauge freedom to set φ_{-n} to be real and positive, and then use (B.4) to solve for φ_{-n} as $\varphi_{-n} = \sqrt{(|\varphi_1|^2 + r)/n}$. We then plug this solution into the kinetic terms

$$\frac{1}{2\pi} \int d^2\sigma (-\mathcal{D}^\mu \varphi_1 \mathcal{D}_\mu \varphi_1 - \mathcal{D}^\mu \varphi_{-n} \mathcal{D}_\mu \varphi_{-n}), \quad (\text{B.5})$$

(where $\mathcal{D}_\mu \varphi_1$, $\mathcal{D}_\mu \varphi_{-n}$ are the usual covariant derivatives) and classically integrate out³⁵ the gauge boson v_μ (see subsection B.7 for the details). We find that the dynamics in this limit is governed by the flat sigma model $S = \frac{1}{2\pi} \int d^2\sigma (\partial_\mu \varphi_1 \partial^\mu \bar{\varphi}_1)$. Note, however, that our gauge choice leaves unfixed a residual \mathbf{Z}_n group of gauge transformations, generated by

$$\varphi_1 \rightarrow e^{2\pi i/n} \varphi_1, \quad (\text{B.6})$$

consequently, the low energy physics of our GLSM in the UV limit is the supersymmetric sigma model on \mathbf{C}/\mathbf{Z}_n .

B.6. Deviations from the UV Fixed Point

Next we consider the deformation of the UV sigma model as r decreases away from infinity, but is still very large $r \gg 1$. As the GLSM has $\mathcal{N} = 2$ worldsheet supersymmetry for all values of r , the corresponding deviation in the sigma model must correspond to adding a linear combination of the chiral operators to the worldsheet Lagrangian. The correct deformation turns out to be

$$\int d^2z e^{-\frac{r+i\theta}{n}} V_T, \quad (\text{B.7})$$

where V_T is the lowest dimensional tachyon vertex operator in the first twisted sector. In order to see this identification more clearly, note that, when $r \gg 1$, (B.1) has fractional instantons (vortices in which the vev of φ_n winds at infinity [23]). Any Euclidean correlation

³⁵ When r is very large the classical approximation is valid as (according to (B.4)) φ_{-n} is also very large in this limit, and so the gauge boson is very massive, by the Higgs mechanism - recall the gauge theory is free in the UV).

function in the theory (B.1) may be represented as a sum over sectors containing arbitrary numbers of instantons and anti instantons; each instanton must also be integrated over the world sheet. On flowing to low energies, these fractional instantons become twist fields (recall that the phase of φ_1 changes by $\frac{2\pi}{n}$ on circling a fractional instanton). The sum over all numbers and positions of instantons and anti-instantons is thus achieved by perturbing the low energy sigma model by (B.7), where the coefficient of V_T is the action of a single instanton.

B.7. Classical RG flow to the IR

In this subsection we will compute the sigma model metric corresponding to \mathbf{C}/\mathbf{Z}_n RG flow, in the classical approximation described in subsection 3.2 above.

First we assume that r is positive and solve the D-term condition (B.4) as follows

$$\varphi_1 = \rho e^{i\theta_1}, \quad \varphi_{-n} = \sqrt{\frac{\rho^2 + r}{n}} e^{i\theta_n}, \quad (\text{B.8})$$

where the $U(1)$ gauge transformation (3.2) acts as $(\theta_n, \theta_1) \sim (\theta_n - n\alpha, \theta_1 + \alpha)$. Then the kinetic terms of the scalar field action become

$$L = (\partial_\mu \rho)^2 + \rho^2 (\partial_\mu \theta_1 - v_\mu)^2 + \frac{\rho^2}{n(\rho^2 + r)} (\partial_\mu \rho)^2 + \frac{\rho^2 + r}{n} (\partial_\mu \theta_n + n v_\mu)^2. \quad (\text{B.9})$$

The equation of motion of the gauge field in the sigma model limit $e \rightarrow \infty$ leads to

$$v_\mu = \frac{\rho^2 \partial_\mu \theta_1 - (\rho^2 + r) \partial_\mu \theta_n}{(n+1)\rho^2 + nr}. \quad (\text{B.10})$$

After we integrate out the vector field, we get

$$L = \left(1 + \frac{\rho^2}{n(\rho^2 + r)}\right) (\partial_\mu \rho)^2 + \frac{\rho^2(\rho^2 + r)}{n((n+1)\rho^2 + nr)} (\partial_\mu \theta)^2, \quad (\text{B.11})$$

where we have defined the gauge invariant field $\theta = n\theta_1 + \theta_n$ ($\theta \sim \theta + 2\pi$). In the UV limit $r \rightarrow \infty$ (or $r \gg \rho$) this sigma model corresponds to the metric of \mathbf{C}/\mathbf{Z}_n

$$ds^2 = d\rho^2 + \frac{\rho^2}{n^2} d\theta^2. \quad (\text{B.12})$$

In the region $\rho \gg r$ we obtain the metric of $\mathbf{C}/\mathbf{Z}_{n+1}$

$$ds^2 = \frac{n+1}{n}d\rho^2 + \frac{\rho^2}{n(n+1)}d\theta^2. \quad (\text{B.13})$$

As we argue in section 4.2, the appearance of $\mathbf{C}/\mathbf{Z}_{n+1}$ is due to our classical approximation and the quantum correction should modify it such that asymptotic geometry is given by \mathbf{C}/\mathbf{Z}_n .

Next we consider the case of negative r . The solution to the D-term condition is given by

$$\varphi_1 = \sqrt{n\rho'^2 + |r|}e^{i\theta_1}, \quad \varphi_{-n} = \rho'e^{i\theta_n}. \quad (\text{B.14})$$

By using the same method as before we obtain the gauge field

$$v_\mu = \frac{(|r| + n\rho'^2)\partial_\mu\theta_1 - n\rho'^2\partial_\mu\theta_n}{n(n+1)\rho'^2 + |r|}, \quad (\text{B.15})$$

and the sigma model metric

$$ds^2 = \left(1 + \frac{n^2\rho'^2}{|r| + n\rho'^2}\right)d\rho'^2 + \frac{\rho'^2(n\rho'^2 + |r|)}{n(n+1)\rho'^2 + |r|}d\theta^2. \quad (\text{B.16})$$

In the IR limit $r \rightarrow -\infty$ (or $|r| \gg \rho'$) we obtain the metric of \mathbf{C}

$$ds^2 = d\rho'^2 + \rho'^2d\theta^2. \quad (\text{B.17})$$

On the other hand, in the far region $\rho' \gg |r|$, the metric looks like $\mathbf{C}/\mathbf{Z}_{n+1}$

$$ds^2 = (n+1)d\rho'^2 + \frac{\rho'^2}{n+1}d\theta^2. \quad (\text{B.18})$$

B.8. Qualitative Properties of the Exact Flow

The evolution of the sigma model metric behind occurs in two stages. When $r > 0$, the metric remains almost constant. More precisely \mathbf{C}/\mathbf{Z}_n is deformed to $\mathbf{C}/\mathbf{Z}_{n+1}$ at very large distances; in (B.11) this deformation propagates inwards. This propagation is clearly reversed by quantum corrections (a bubble of \mathbf{C}/\mathbf{Z}_n immersed in $\mathbf{C}/\mathbf{Z}_{n+1}$ grows rather than shrinks in worldsheet RG flow [1], [18].), and is an artifact of our approximation; in the quantum corrected RG flow we expect the metric to stay constant for $r > 0$.

As r turns negative, however, (B.16) describes a bubble of flat space which is nucleated at $\rho = 0$. This bubble then expands out in a diffusive manner; its radius grows like $R \sim \sqrt{r} \sim \sqrt{(n-1)\ln\Lambda}$, in rough agreement with the one loop sigma model growth discussed in [1], [18]. Consequently, the evolution of the sigma model described behind (together with the minor expected quantum corrections) is summarized in Fig. 6, and is in perfect agreement with the APS picture reviewed in B.1.

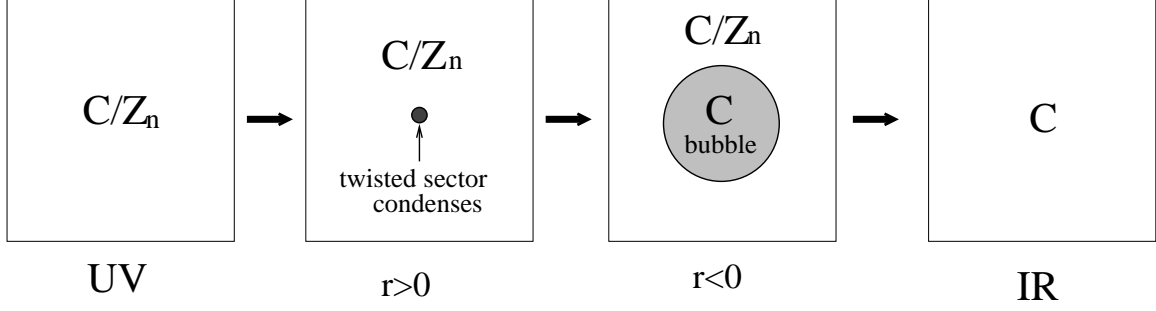


Fig. 6: Change of geometry under closed string tachyon in C/Z_n .

Appendix C. Classical Metric in Twisted Circle GLSM

As in Appendix B, let us compute the classical metric of the gauged linear sigma model in section 4.3, which has the kinetic terms

$$L_{kin} = \frac{k}{2}(\partial_\mu P_1)^2 + \frac{k}{2}(\partial_\mu P_2 + v_\mu)^2 + (\partial_\mu \rho)^2 + \rho^2(\partial_\mu \theta_1 + v_\mu)^2 + (\partial_\mu \rho')^2 + \rho'^2(\partial_\mu \theta_n - n v_\mu)^2, \quad (C.1)$$

and the D-term condition $n\rho'^2 - \rho^2 = kP_1$ (or (3.3)). Just in the same way as in B.7 we can integrate out the gauge field. After we impose the gauge fixing condition $\theta_n = 0$ from the beginning (just for simplicity)

$$v_\mu = -\frac{\rho^2 \partial_\mu \theta_1 + \frac{k}{2} \partial_\mu P_2}{\rho^2 + n^2 \rho'^2 + \frac{k}{2}}, \quad (C.2)$$

we get the sigma model metric

$$ds^2 = (d\rho)^2 + (d\rho')^2 + \frac{k}{2}(dP_1)^2 + \frac{\rho^2(n^2 \rho'^2 + \frac{k}{2})(d\theta_1)^2 - k\rho^2 d\theta_1 dP_2 + \frac{k}{2}(\rho^2 + n^2 \rho'^2)(dP_2)^2}{\rho^2 + n^2 \rho'^2 + \frac{k}{2}}. \quad (C.3)$$

First we assume $P_1 > 0$ then we have ($\rho \equiv |\varphi_1|$)

$$ds^2 = (d\rho)^2 + \frac{k}{2}(dP_1)^2 + \frac{(\rho d\rho + \frac{k}{2} dP_1)^2}{n(\rho^2 + kP_1)} + \frac{(n\rho^4 + (nkP_1 + \frac{k}{2})\rho^2)(d\theta_1)^2 - k\rho^2(d\theta_1)(dP_2) + \frac{k}{2}((n+1)\rho^2 + nkP_1)(dP_2)^2}{(n+1)\rho^2 + nkP_1 + \frac{k}{2}}. \quad (C.4)$$

In the UV limit $\rho \ll kP_1$ we obtain

$$ds^2 = (d\rho)^2 + \rho^2(d\theta_1)^2 + \frac{k}{2}(dP_1)^2 + \frac{k}{2}(dP_2)^2, \quad (C.5)$$

which is equivalent to the twisted circle $\mathbf{C} \times \mathbf{S}^1/\mathbf{Z}_n$ after we take the remained \mathbf{Z}_n gauge equivalence $(\theta_1, P_2) \sim (\theta_1 + \frac{2\pi}{n}, P_2 + \frac{2\pi}{n})$ into account. On the other hand in the opposite limit $\rho^2 \gg kP_1$ we get

$$ds^2 \simeq \frac{n+1}{n}(d\rho)^2 + \frac{n}{n+1}\rho^2(d\theta_1)^2 + \frac{k}{2}(dP_1)^2 + \frac{k}{2}(dP_2)^2 - \frac{k}{n+1}d\theta_1 dP_2, \quad (\text{C.6})$$

which may be described by a twisted circle $(\mathbf{C} \times \mathbf{S}^1)/\mathbf{Z}_{n+1}$. This geometry is also argued to be an artifact of the classical approximation. If we take the quantum correction into account, the asymptotic region should always be the previous twisted circle $(\mathbf{C} \times \mathbf{S}^1)/\mathbf{Z}_n$.

Finally in the case of $P_1 < 0$ the result is given by ($\rho' \equiv |\varphi_{-n}|$)

$$ds^2 = (d\rho')^2 + \frac{k}{2}(dP_1)^2 + \frac{(n\rho'd\rho' + \frac{k}{2}dP_1)^2}{n\rho'^2 + kP_1} + \frac{(n^2\rho'^2 + \frac{k}{2})(n\rho'^2 + kP_1)(d\theta_1)^2 - k(n\rho'^2 + kP_1)(d\theta_1)(dP_2) + \frac{k}{2}(n(n+1)\rho'^2 + kP_1)(dP_2)^2}{n(n+1)\rho'^2 + kP_1 + \frac{k}{2}}. \quad (\text{C.7})$$

If we take the limit $\rho'^2 \ll k|P_1|$, then the metric becomes

$$ds^2 = d\rho'^2 + n^2\rho'^2 d\theta_1^2 + \frac{k}{2}(dP_2 - d\theta_1)^2, \quad (\text{C.8})$$

and thus we get the flat space $\mathbf{C} \times \mathbf{S}^1$. This gives the bubble of flat space. It is also easy to see that the opposite limit $\rho'^2 \gg k|P_1|$ corresponds to $(\mathbf{C} \times \mathbf{S}^1)/\mathbf{Z}_{n+1}$ as before.

Appendix D. D-brane Spectrum in dual LG Theory

D.1. LG Theory dual to GLSM

In [47] Hori and Vafa have argued that a gauge linear sigma model with p different matter chiral multiplets is exactly dual to a Landau Ginzburg model of $p+1$ interacting twisted chiral multiplets. The first of these twisted chiral multiplets is simply the gauge multiplet Σ . The remaining twisted chiral multiplets are obtained as follows. Each of the chiral multiplets of the GLSM may be written as $\varphi_i = e^{\psi_i}$, where the imaginary part of ψ_i is periodic with period 2π . We now, roughly, T-dualize this GLSM with respect to each of these periodic variables. The dual angular coordinate pairs up with the real part of ψ and

the original fermions to form a twisted chiral multiplet Y_i ³⁶. While the imaginary part of Y_i is a gauge invariant and supersymmetrized version of the T-dual of the imaginary part of ψ , it turns out that the real part of the twisted chiral multiplet is given by $Y_i + \bar{Y}_i = 2\bar{\varphi}_i e^{2QV} \varphi_i$ (see eqns 3.18-3.19, [47], for more details). The twisted superpotential for these fields that follows from the usual T-duality arguments is $\Sigma(\sum_i Q_i Y_i - t)$ where Q_i are the charges of the fields φ_i . In addition to this classical contribution, the twisted chiral potential also receives instanton (vortex) contributions; as shown in [47] the exact quantum corrected twisted superpotential is the classical piece plus $\sum_i e^{Y_i}$.

The kinetic terms for these twisted chiral multiplets Y_i and σ cannot be computed exactly. However, classically, at low energies ($e \rightarrow \infty$) integrating the σ field out simply results in the constraint $\sum_i Q_i Y_i + t = 0$ on the Y_i fields. This constraint, the mirror of the GLSM D term equation, is expected to be exact at low energies. Consequently, the low energies, we have the Landau Ginzburg theory of a $p - 1$ twisted chiral multiplets (Y_i subject to the constraint described above) and the twisted chiral superpotential $\sum_i e^{Y_i}$.

Now let us apply this procedure to the GLSM (B.1) for \mathbf{C}/\mathbf{Z}_n in appendix B and its Liouville version (for twisted circle) in section 3.1. Performing the mirror transformation we obtain the following LG potential for the former model [3]

$$W = e^{-Y_1} + e^{-Y_2} = e^{-nU} + e^{-t/n-U}, \quad (\text{D.1})$$

where Y_1 and Y_2 are dual to φ_1 and φ_{-n} satisfying the relation $-Y_1 + nY_2 = t$. In other words, we can write $Y_1 (= nU) = |\varphi_1|^2 + i\phi_1$, $Y_2 = |\varphi_{-n}|^2 + i\phi_{-n}$, where the phases ϕ_1 and ϕ_{-n} are dual to θ_1 and θ_n . The periodicity of these fields $Y_{1,2} \sim Y_{1,2} + 2\pi i$ leads³⁷ to the identification $U \sim U + 2\pi i$. Note that we can see the symmetry $\text{Im}t(=\theta) \rightarrow \text{Im}t + 2\pi i$ by considering the accompanied field redefinition $U \rightarrow U - 2\pi i/n$.

³⁶ This follows from the fact that T-duality reverses the sign of the left moving part of the angular variable; this exchanges the left moving part of ψ_i with its complex conjugate, but has no such effect on the right moving part.

³⁷ Here we used the constraint $-Y_1 + nY_2 = t$ and thus the periodicity of U is not $2\pi i/n$ but $2\pi i$.

Now let us consider the change of geometry from the viewpoint of the LG theory. Before the tachyon condensation ($r \rightarrow \infty$), we obtain the simple potential

$$W = e^{-nU}, \quad (\text{D.2})$$

and this has the \mathbf{Z}_n quantum symmetry

$$h : U \rightarrow U + 2\pi i/n, \quad (\text{D.3})$$

which corresponds to the previous quantum symmetry (2.5) in GLSM. Indeed this potential is the same as the large radius limit ($k \rightarrow \infty$) of the model [24] and can be identified with the orbifold \mathbf{C}/\mathbf{Z}_n . The closed string tachyon condensation is represented by the second term of (D.1) and breaks this symmetry. This term represents the fractional instanton (vortex) effect in GLSM and is consistent with our arguments around (B.7). The final state after tachyon condensation can be regarded as the flat space \mathbf{C} as the potential $W \sim e^{-U}$ shows in the $t \rightarrow -\infty$ limit.

It is also possible to perform the mirror transformation for the model discussed in section 3.1 by using the method in [24]. Then we obtain the LG potential [7]

$$W = e^{-nU} + e^{-Y_P/n-U}, \quad (\text{D.4})$$

where the fields Y_P denote the dual twisted chiral field of P . One may ask how we can see the (dual of) twisted identification of $\mathbf{C}/\mathbf{Z}_n \times \mathbf{S}^1$ for the large P_1 . This is understood as follows. Because we have the periodicity 2π for each of the imaginary parts of Y_P, Y_1 and Y_2 with the constraint $-Y_1 + nY_2 = Y_P$, we find not only the periodicity $U \sim U + 2\pi i\mathbf{Z}$ and $Y_p \sim Y_p + 2n\pi i\mathbf{Z}$ but also the \mathbf{Z}_n identification

$$(U, Y_P) \sim (U + 2\pi i/n, Y_P - 2\pi i). \quad (\text{D.5})$$

This projection (D.5) just corresponds to the twisted identification (see Appendix E). Because of this monodromy the true radius is $\tilde{R}_{UV} = \frac{n\sqrt{\alpha'}}{\sqrt{k}}$. Thus it is obvious that we obtain the twisted circle in the UV limit. On the other hand, in the IR limit the dominant term becomes the second term and thus we get the flat space³⁸.

³⁸ If we consider P_1 takes a large negative value, then we should use the good variables Y_1, Y_p as $W = e^{-nY_1+Y_p} + e^{-Y_1}$ and thus we have no such twisted identification ($\tilde{R}_{IR} = \sqrt{\frac{\alpha'}{k}}$).

D.2. Description of D-branes in LG Theory dual to Orbifold

In this subsection we will investigate the D-brane spectrum of \mathbf{C}/\mathbf{Z}_n in the dual Landau Ginzburg model (D.2). We will use the constraints from $\mathcal{N} = 2$ supersymmetry [15][48] in what follows.

We concentrate on D1-branes which preserve the A-type supersymmetry (A-brane). The general arguments of [15][48], demonstrate that such D-branes have a (middle dimensional) Lagrangian sub manifold as their world-volume; further the imaginary part of the superpotential is constant along this world-volume. The first condition is satisfied by any curve in the U plane. The second one is crucial and is less easily satisfied. We first consider the 1-branes that are mirror (T-dual) to the GLSM D2-branes $|m\rangle_{D2}$ of subsection 4.1. Note that we T-dualize along the $\text{Im}U$ direction to map between these pictures, consequently the branes we are after are localized in the $\text{Im}U$ direction. They are given by

$$\text{Im}U = \frac{2\pi im}{n}, \tag{D.6}$$

where the numbers $m = 0, 1, \dots, n - 1$ label the types of D1-branes⁴⁰. We denote this world-volume (D.6) by γ_m (see Fig.7 below). Indeed the \mathbf{Z}_n quantum symmetry action $h : \text{Im}U \rightarrow \text{Im}U + 2\pi i/n$ generates the other D1-branes in the same way as in GLSM.

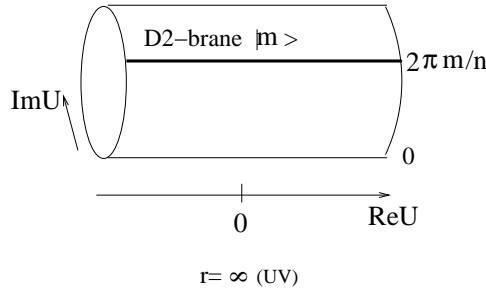


Fig. 7: The LG description of D2-brane.

³⁹ Even though one can consider other possibilities of curved world-line, they do not satisfy the boundary conformal invariance in the UV limit.

⁴⁰ One may note that the supersymmetric condition allows the half-integer value of m . There are related to integer m by the operation $(-1)^{FL} : U \rightarrow -U$. Since the boundary state is invariant under GSO projection $\frac{1+(-1)^{FL}}{2}$, we should add the brane $m + n/2$ to m in (D.6). This complication does not change our arguments later and we will not explicitly mention it below.

We now turn to a discussion of D1-branes that are dual to D0-branes. The direct determination of such branes is complicated by the following fact. The Landau Ginzburg model that reduces to \mathbf{C}/\mathbf{Z}_n has vanishing kinetic term (this is the $k \rightarrow \infty$ limit in [24]). The Liouville potential, is, consequently effectively infinite when $\text{Re}U$ is negative, and is effectively zero when $\text{Re}U$ is positive. For any finite value of the the LG kinetic term (if k in [24] is not strictly infinite), the wrapped 1-branes of the Landau Ginzburg model (D.1) are attracted to, and stuck at, the strong coupling region. Strictly in the $k \rightarrow \infty$ limit this 1-brane is free to wander in the bulk. Thus we do not expect to find any \mathbf{C}/\mathbf{Z}_n brane, localized in the $\text{Re}U$ direction, using the usual Landau Ginzburg techniques (which work when the LG kinetic term is nonsingular). Nonetheless it is not difficult to build a qualitative picture of the states we expect.

As discussed in section 5, GLSM 0-branes may be obtained from GLSM $D2 - \overline{D2}$ by the open string tachyon condensation. A bulk D0-brane is a vortex on a D2 and an anti D2-brane of the same sort; consequently it is natural to conjecture that the world volume of such a brane is a circle along the $\text{Im}U$ direction (see the left-hand side of Fig.8). Indeed it has the correct D0-brane charge after the T-duality and is obviously movable away from the fixed point in the $k \rightarrow \infty$ limit⁴¹. On the other hand, we can generate a fractional D0-brane $|m\rangle_{D0}$ from a D2 $|m+1\rangle_{D2}$ and a $\overline{D2}$ $|\bar{m}\rangle_{\overline{D2}}$. In this case we argue that its world-volume after the open string tachyon condensation is (approximately) given by (see the right-hand side of Fig.8)

$$\{U = x \mid x < 0\} \cup \left\{U = \frac{2\pi im}{n} + i\theta \mid 0 \leq \theta \leq \frac{2\pi}{n}\right\} \cup \{U = y + \frac{2\pi i}{n} \mid y < 0\}. \quad (\text{D.7})$$

It seems reasonable that annihilation (open string tachyon condensation) of the $|\bar{m}\rangle_{\overline{D2}}$ occurs only for positive $\text{Re}U$ because the existence of the Liouville potential; thus this open string tachyon condensation leaves behind a remnant stuck at $U = 0$; this remnant is the T-dual of the fractional 0-brane. Note, of course, that it winds a fraction of the $\text{Im}U$ circle.

⁴¹ One may think that this configuration of a D0-brane breaks the A-type supersymmetry because it does not satisfies the condition of superpotential mentioned before. However, our non-compact orbifold corresponds to the limit of vanishing the kinetic term of the Liouville theory as we have noted. Thus the Liouville potential can be neglected for $\text{Re}U > 0$ and it will keep the A-type supersymmetry. This is also equivalent to the fact that the dilaton is constant in the limit $k \rightarrow \infty$.

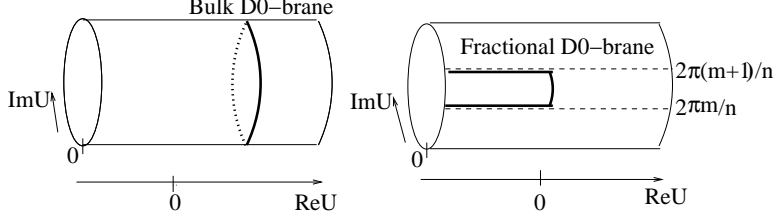


Fig. 8: The LG description of D0-brane.

D.3. Computation of RR-charges

To check these interpretations, let us compute the coupling to the RR-sector ground state by using the information of superpotential.

In the papers [15][48] D1-branes in the LG theory of $W = \Phi^{k+2}$, which is equivalent to the $\mathcal{N} = 2$ minimal model in the IR limit, were analyzed and we can use this result by performing the change of the variable $\Phi \rightarrow e^{-U}$.

First we start with the D1-brane given by (D.6). The couplings to the k^{th} twisted RR-sector ground state ($\mathcal{N} = 2$ chiral state) can be expressed ⁴² by the following ‘boundary state’

$$|m\rangle_{D2} = \sum_{k=0}^{n-1} \frac{c_{k,m}^0}{N_k} |e^{-kU}\rangle, \quad (\text{D.8})$$

where we can compute the coefficient $c_{k,m}^0$ as follows

$$\begin{aligned} c_{k,m}^0 &= \int_{\gamma_m} dU e^{-kU} e^{-W} \\ &= e^{-2\pi i m k/n} \int_{-\infty}^{\infty} dx e^{-kx} e^{-e^{-nx}} = \frac{e^{-2\pi i m k/n}}{n} \Gamma(k/n). \end{aligned}$$

The normalization N_k of the RR-sector ground state $|e^{-kU}\rangle$ can also be determined by using the intersection number (see the later arguments and also [15](p.50) for more detail)

$$N_k = \langle \overline{e^{-kU}} | e^{-kU} \rangle = \frac{2 \sin(\pi k/n)}{n} \Gamma(k/n)^2. \quad (\text{D.10})$$

Thus we get the normalized couplings

$$c_{k,m}(\equiv \frac{c_{k,m}^0}{\sqrt{N_k}}) = \frac{1}{\sqrt{2n \sin(\pi k/n)}} e^{-2\pi i m k/n}. \quad (\text{D.11})$$

⁴² Here the sector $k = 0$ corresponds to the untwisted sector and its coefficient is divergent due to the infinite volume. Below we can omit this sector because it does not contribute to the present calculations.

This result matches exactly with the D2-brane boundary state in the orbifold theory [43] including the normalization.

Next we turn to D1-branes which are dual to D0-branes in GLSM. Their couplings to the RR-sector ground states $c'_{k,\alpha}$ do not change under open string tachyon condensation and thus we can compute it as follows

$$c'_{k,m} = c_{k,m+1} - c_{k,m} = \sqrt{\frac{2 \sin(\pi k/n)}{n}} e^{-\pi i(k/n+1/2)} \cdot e^{-2\pi i m k/n}. \quad (\text{D.12})$$

Thus we again find the exact agreement with the result of the boundary states in the orbifold theory [36] [37] up to an irrelevant phase factor. Note also that the intersection numbers $I_{m,m'}$ (or equally open string Witten index $\text{Tr}_R(-1)^F$ [49]) of these D1-branes are given by the overlap of the two boundary state with the insertion⁴³ of $(-1)^{F_L} = ie^{\pi i k}$ as follows

$$\begin{aligned} \langle m | (-1)^{F_L} | m' \rangle_{D0} &= \sum_{k=1}^{n-1} i e^{\pi i k/n} \cdot \frac{2 \sin(\pi k/n)}{n} \cdot e^{\frac{2\pi i}{n}(m-m')} \\ &= \delta_{m,m'+1} - \delta_{m,m'+l+1}, \end{aligned}$$

and indeed reproduce the quiver theory result⁴⁴.

D.4. Speculations on D-branes in the LG Model

Consider the LG dual to the \mathbf{C}/\mathbf{Z}_n 2-brane $|0\rangle$ described in subsection 4.2. As we have described above, the Landau Ginzburg description of this state is a 1-brane located at $\text{Im}U=0$ (assuming $\theta = 0$). In fact $\text{Im}U=0$ continues to preserve $\mathcal{N} = 2$ supersymmetry even upon turning on the tachyon superpotential in (D.1); so the mirror to $|0\rangle$ evolves into the mirror of a bulk 2-brane in flat space, in agreement with our previous results.

The situation is not as simple for other 2-branes in (D.6). On turning on the tachyon contribution to (D.1), the world line of these branes begins to bend inwards towards $\text{Im}U=0$ (see Fig. 9) (this follows from the condition that the imaginary part of the superpotential

⁴³ In the case of $\mathcal{N} = 2$ minimal model we should take $(-1)^{F_L} = ie^{\pi i k/n}$ and the index is slightly different from our model.

⁴⁴ This is easy to see from the fact that the \mathbf{Z}_n projection is given by $e^{\frac{2\pi i}{n}(m-m')} \cdot e^{\frac{2\pi i(n+1)}{n}s_1} = 1$, where $s_1 = \pm \frac{1}{2}$ is the (spacetime) spin of fermionic ground states in \mathbf{C}/\mathbf{Z}_n .

remain constant). However, as the closed string tachyon is localized, at any finite r the effect of tachyon condensation should be restricted to the region $\text{Re}U \approx \sqrt{|r|}$. Consequently the world line of the 1-brane may be expected to curve back up to its initial value (see the right end of Fig. 9). This configuration naively breaks $\mathcal{N} = 2$ worldsheet supersymmetry, but, as in subsection D.2, this breaking may vanish in the $k \rightarrow \infty$ limit. If these speculations are indeed true, they would also explain the disappearance of the fractional 0-branes (D.7) under tachyon condensation. However we leave the verification (or otherwise) of these speculations to future work.

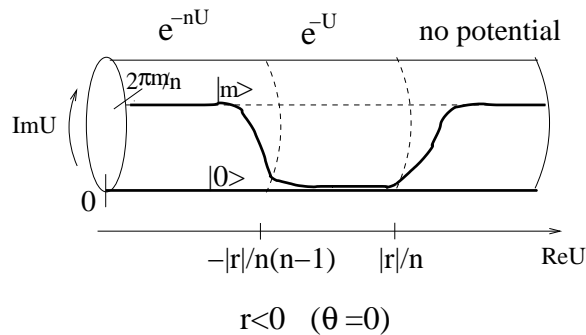


Fig. 9: The D2-brane in LG description after the RG-flow. We show the world-volume of both D2-branes $|m\rangle_{D2}$ and $|0\rangle_{D2}$. Even though the former D2-brane will be deformed for $-|r|/n(n-1) < \text{Re}U < |r|/n$, where the Liouville potential e^{-U} dominates the superpotential, it does not change in the asymptotic region $\text{Re}U > |r|/n$. Finally we can see that in the limit $r \rightarrow -\infty$ all these fractional D2-branes will become the same usual D2-brane in flat space. (In this picture we assumed $\theta = 0$ for simplicity.)

Appendix E. Useful T-duality Relations

Here we would like to summarize the various T-dual expressions of the twisted circle $(\mathbf{C} \times \mathbf{S}^1)/\mathbf{Z}_n$ model. We denote the \mathbf{Z}_n projection by $g = \exp(\frac{2\pi i(n+1)}{n}J_{12})$ and its dual \mathbf{Z}_n quantum symmetry⁴⁵ by h (2.5). The $1/n$ shift is also represented by $\sigma_{1/n}$ and its dual operator by $\tilde{\sigma}_{1/n}$. Then we obtain the following equivalent descriptions

$$\text{IIA(B) Melvin Model (radius } R \text{ and } \zeta(=qR) = (n+1)/n) \quad (\text{E.1a})$$

⁴⁵ Note that this includes a particular example of $g = (-1)^{FS}$ and $h = (-1)^{FL}$ for $\mathcal{N} = 2$ (see also [30], [22], [1]).

$$\simeq \text{IIA(B) on } [\mathbf{C} \times \mathbf{S}^1 \text{ (radius } nR)] / (g \cdot \sigma_{1/n}) \text{ (= twisted circle)} \quad (\text{E.1b})$$

$$\simeq \text{IIA(B) on } [\mathbf{C}/\mathbf{Z}_n \times \mathbf{S}^1 \text{ (radius } R)] / (h \cdot \tilde{\sigma}_{1/n}) \quad (\text{E.1c})$$

$$\simeq \text{IIB(A) Melvin Model (radius } 1/R \text{ and } \beta\alpha'R = (n+1)/n) \quad (\text{E.1d})$$

$$\simeq \text{IIB(A) on } [\mathbf{C} \times \mathbf{S}^1 \text{ (radius } 1/nR)] / (g \cdot \tilde{\sigma}_{1/n}) \quad (\text{E.1e})$$

$$\simeq \text{IIB(A) on } [\mathbf{C}/\mathbf{Z}_n \times \mathbf{S}^1 \text{ (radius } 1/R)] / (h \cdot \sigma_{1/n}), \quad (\text{E.1f})$$

where the parameter β corresponds to the B-field flux T-dual to the twisted parameter $q = \zeta/R$ (see [6][14]). These are all explained as T-duality relations.

Finally let us consider the relation to LG theory. As we have seen, the UV region ($Y_p \rightarrow \infty$) of the LG theory (D.4) is equivalent to the twisted circle. This is understood in the above picture as follows. This LG theory is defined by the superpotential (D.2), which is equivalent to the orbifold \mathbf{C}/\mathbf{Z}_n , and by the twisted identification (D.5)

$$\text{typeIIA(B) on } [\mathbf{C}/\mathbf{Z}_n \times \mathbf{S}^1 \text{ (radius } 1/R)] / (g' \cdot \sigma_{1/n}), \quad (\text{E.2})$$

where the \mathbf{Z}_n action g' denotes the shift $U \rightarrow U + 2\pi i/n$. If we take T-duality in the angular direction of \mathbf{C} , then we have the projection h instead of g' . Therefore this model is indeed equivalent to the expression (E.1f).

References

- [1] A. Adams, J. Polchinski and E. Silverstein, “Don’t panic! Closed string tachyons in ALE space-times,” JHEP **0110** (2001) 029 [arXiv:hep-th/0108075].
- [2] A. Dabholkar, “Tachyon condensation and black hole entropy,” arXiv:hep-th/0111004.
- [3] C. Vafa, “Mirror symmetry and closed string tachyon condensation,” arXiv:hep-th/0111051; A. Dabholkar and C. Vafa, “ tt^* geometry and closed string tachyon potential,” JHEP **0202** (2002) 008 [arXiv:hep-th/0111155].
- [4] J. A. Harvey, D. Kutasov, E. J. Martinec, G. Moore, “Localized tachyons and RG flows”, arXiv:hep-th/0111154.
- [5] E. J. Martinec, “Defects, decay, and dissipated states,” arXiv:hep-th/0210231.
- [6] J. G. Russo and A. A. Tseytlin, “Magnetic flux tube models in superstring theory,” Nucl. Phys. B **461**, 131 (1996) [arXiv:hep-th/9508068].
- [7] J. R. David, M. Gutperle, M. Headrick and S. Minwalla, “Closed string tachyon condensation on twisted circles,” JHEP **0202**, 041 (2002) [arXiv:hep-th/0111212].
- [8] M. Gutperle and A. Strominger, “Fluxbranes in string theory,” JHEP **0106** (2001) 035 [arXiv:hep-th/0104136].
- [9] J. G. Russo and A. A. Tseytlin, “Magnetic backgrounds and tachyonic instabilities in closed superstring theory and M-theory,” Nucl. Phys. B **611**, 93 (2001) [arXiv:hep-th/0104238].
- [10] T. Suyama, “Properties of string theory on Kaluza-Klein Melvin background,” JHEP **0207**, 015 (2002) [arXiv:hep-th/0110077].
- [11] M. Gutperle, “A note on perturbative and nonperturbative instabilities of twisted circles,” Phys. Lett. B **545**, 379 (2002) [arXiv:hep-th/0207131].
- [12] J. R. David, “Unstable magnetic fluxes in heterotic string theory,” JHEP **0209**, 006 (2002) [arXiv:hep-th/0208011].
- [13] E. J. Martinec and G. Moore, “On decay of K-theory,” arXiv:hep-th/0212059.
- [14] T. Takayanagi and T. Uesugi, “Orbifolds as Melvin geometry,” JHEP **0112** (2001) 004 [arXiv:hep-th/0110099].
- [15] K. Hori, A. Iqbal and C. Vafa, “D-branes and mirror symmetry,” arXiv:hep-th/0005247.
- [16] S. Govindarajan, T. Jayaraman and T. Sarkar, “On D-branes from gauged linear sigma models,” Nucl. Phys. B **593**, 155 (2001) [arXiv:hep-th/0007075].
- [17] K. Hori, “Linear models of supersymmetric D-branes,” arXiv:hep-th/0012179.
- [18] M. Gutperle, M. Headrick, S. Minwalla and V. Schomerus, “Space-time energy decreases under world-sheet RG flow,” arXiv:hep-th/0211063.
- [19] A. A. Tseytlin, “Melvin solution in string theory,” Phys. Lett. B **346**, 55 (1995) [arXiv:hep-th/9411198].

- [20] A. A. Tseytlin, “Closed superstrings in magnetic flux tube background,” Nucl. Phys. Proc. Suppl. **49**, 338 (1996) [arXiv:hep-th/9510041].
- [21] C. Vafa, “Quantum Symmetries Of String Vacua,” Mod. Phys. Lett. A **4**, 1615 (1989).
- [22] M. S. Costa and M. Gutperle, “The Kaluza-Klein Melvin solution in M-theory,” JHEP **0103** (2001) 027 [arXiv:hep-th/0012072].
- [23] E. Witten, “Phases of $N = 2$ theories in two dimensions,” Nucl. Phys. B **403**, 159 (1993) [arXiv:hep-th/9301042].
- [24] K. Hori and A. Kapustin, “Duality of the fermionic 2d black hole and $N = 2$ Liouville theory as mirror symmetry,” JHEP **0108** (2001) 045 [arXiv:hep-th/0104202].
- [25] T. Takayanagi and T. Uesugi, “D-branes in Melvin background,” JHEP **0111** (2001) 036 [arXiv:hep-th/0110200]; T. Takayanagi and T. Uesugi, “Flux stabilization of D-branes in NSNS Melvin background,” Phys. Lett. B **528** (2002) 156 [arXiv:hep-th/0112199].
- [26] E. Dudas and J. Mourad, “D-branes in string theory Melvin backgrounds,” Nucl. Phys. B **622** (2002) 46 [arXiv:hep-th/0110186].
- [27] Y. Michishita and P. Yi, “D-brane probe and closed string tachyons,” Phys. Rev. D **65**, 086006 (2002) [arXiv:hep-th/0111199].
- [28] M. R. Douglas and G. W. Moore, “D-branes, Quivers, and ALE Instantons,” arXiv:hep-th/9603167.
- [29] D. E. Diaconescu, M. R. Douglas and J. Gomis, “Fractional branes and wrapped branes,” JHEP **9802** (1998) 013 [arXiv:hep-th/9712230].
- [30] O. Bergman and M. R. Gaberdiel, “Dualities of type 0 strings,” JHEP **9907** (1999) 022 [arXiv:hep-th/9906055].
- [31] E. Witten, “On string theory and black holes,” Phys. Rev. D **44**, 314 (1991).
- [32] S. Hellerman and J. McGreevy, “Linear sigma model toolshed for D-brane physics,” JHEP **0110**, 002 (2001) [arXiv:hep-th/0104100].
- [33] S. Govindarajan and T. Jayaraman, “Boundary fermions, coherent sheaves and D-branes on Calabi-Yau manifolds,” Nucl. Phys. B **618**, 50 (2001) [arXiv:hep-th/0104126].
- [34] S. Hellerman, S. Kachru, A. E. Lawrence and J. McGreevy, “Linear sigma models for open strings,” JHEP **0207** (2002) 002 [arXiv:hep-th/0109069].
- [35] H. Ooguri, Y. Oz and Z. Yin, “D-branes on Calabi-Yau spaces and their mirrors,” Nucl. Phys. B **477** (1996) 407 [arXiv:hep-th/9606112].
- [36] D. E. Diaconescu and J. Gomis, “Fractional branes and boundary states in orbifold theories,” JHEP **0010** (2000) 001 [arXiv:hep-th/9906242].
- [37] M. Billo, B. Craps and F. Roose, “Orbifold boundary states from Cardy’s condition,” JHEP **0101**, 038 (2001) [arXiv:hep-th/0011060].
- [38] C. G. Callan, C. Lovelace, C. R. Nappi and S. A. Yost, “String Loop Corrections To Beta Functions,” Nucl. Phys. B **288**, 525 (1987).

- [39] A. Sen, “Tachyon condensation on the brane antibrane system,” JHEP **9808**, 012 (1998) [arXiv:hep-th/9805170].
- [40] E. Witten, “On background independent open string field theory,” Phys. Rev. D **46** (1992) 5467 [arXiv:hep-th/9208027]; E. Witten, “Some computations in background independent off-shell string theory,” Phys. Rev. D **47** (1993) 3405 [arXiv:hep-th/9210065].
- [41] A. A. Gerasimov and S. L. Shatashvili, “On exact tachyon potential in open string field theory,” JHEP **0010** (2000) 034 [arXiv:hep-th/0009103]; D. Kutasov, M. Marino and G. W. Moore, “Some exact results on tachyon condensation in string field theory,” JHEP **0010** (2000) 045 [arXiv:hep-th/0009148]; D. Kutasov, M. Marino and G. W. Moore, “Remarks on tachyon condensation in superstring field theory,” arXiv:hep-th/0010108.
- [42] P. Kraus and F. Larsen, “Boundary string field theory of the DD-bar system,” Phys. Rev. D **63** (2001) 106004 [arXiv:hep-th/0012198]; T. Takayanagi, S. Terashima and T. Uesugi, “Brane-antibrane action from boundary string field theory,” JHEP **0103** (2001) 019 [arXiv:hep-th/0012210].
- [43] T. Takayanagi, “Holomorphic tachyons and fractional D-branes,” Nucl. Phys. B **603** (2001) 259 [arXiv:hep-th/0103021]; T. Takayanagi, “Tachyon condensation on orbifolds and McKay correspondence,” Phys. Lett. B **519** (2001) 137 [arXiv:hep-th/0106142].
- [44] K. Sugiyama and S. Yamaguchi, “D-branes on a noncompact singular Calabi-Yau manifold,” JHEP **0102**, 015 (2001) [arXiv:hep-th/0011091].
- [45] T. Eguchi and Y. Sugawara, “D-branes in singular Calabi-Yau n-fold and $N = 2$ Liouville theory,” Nucl. Phys. B **598** (2001) 467 [arXiv:hep-th/0011148].
- [46] Y. H. He, “Closed string tachyons, non-supersymmetric orbifolds and generalised McKay correspondence,” arXiv:hep-th/0301162.
- [47] K. Hori and C. Vafa, “Mirror symmetry,” arXiv:hep-th/0002222.
- [48] S. Govindarajan and T. Jayaraman, “On the Landau-Ginzburg description of boundary CFTs and special Lagrangian submanifolds,” JHEP **0007**, 016 (2000) [arXiv:hep-th/0003242].
- [49] M. R. Douglas and B. Fiol, “D-branes and discrete torsion. II,” arXiv:hep-th/9903031.